Exergoeconomic Assessment, Parametric Study and Optimization of a Novel Solar Trigeneration System

A. R. Noorpoor*‡, S.Heidararabi**

*Associate Professor, Mechanical Engineering, Graduate Faculty of Environment, University of Tehran (UT), Tehran, Iran.

**M.Sc. in Energy Systems Engineering, Graduate Faculty of Environment, University of Tehran, Tehran, Iran.

(noorpoor@ut.ac.ir,heidararabi@alumni.ut.ac.ir)

‡Corresponding Author; Ali Reza Noorpoor, Graduate Faculty of Environment, University of Tehran (UT), Tehran, Iran,

Tel: +98 216 647 6132, Fax: +98 216 6401209, noorpoor@ut.ac.ir

Received: 08.03.2016-Accepted:23.07.2016

Abstract-An exergoeconomic analysis is performed for a solar trigeneration system in which the electric power, refrigeration power and domestic hot water are produced by a cascade organic Rankine cycle, an absorption chiller, which is accompanied by ammonia turbine, and a heat recovery cycle respectively, after optimizing the length of PTCs by dynamic modeling analysis. A parametric study is also carried out to investigate the effects of such significant parameters as degree of superheat at the turbine's inlet of power cycle, condenser temperature of power cycle, operating pressure of the refrigerating cycle and operating fluid temperature of the main cycle on the energy and exergy efficiencies and the exergoeconomic performance of the system. Finally a multi objective optimization from the viewpoint of exergoeconomics is reported by using genetic algorithm. As a result of exergoeconomic analysis of the system, ORC Heat Exchanger (ORC Ex), Cooling Tower2 (C.T2), Absorber (Abs) and Reflux Condenser (Ref Cond) exhibit the worst exergoeconomic performance. For the overall system, the capital cost rate, the exergy destruction cost rate and the exergoeconomic factor are calculated to be about 37.98 $/hr, 122.25 $/hr and 23.7%, respectively.

KeywordsSolar trigeneration, Cascade organic Rankine cycle, NH_3/H_2O absorption chiller, Exergoeconomic, Genetic Algorithm, Multi objective optimization.

1. Introduction

The two main concerns for the sustainabilityof energy production in the future are global warming and availability of sources.Despitethe limited availability of non-renewable fuel resources, the demand for energy has been on a steady rise. So far, fossil fuelsare considered and utilized as the eminent source of generating applicable form of energy [1]. On the other side,reference [2] has been estimated that total solar irradiation transmitted to the earth is approximately1.74×10^8 GW, while the total energy consumption of the world is approximately1.84×10^4GW [3]. Thus solar energyperforms the best alternative to reduce the burning of fossil fuels as the International Energy Agency casts that concentrated solar power could provide 11.3% of the overall world electricity production by 2050 [4].

Trigeneration refers to the simultaneous production of cooling, heating, and power. As the literature review in this researchreveals, most of the investigations of trigeneration systemshavebeen done in the last few years. These incrementsof researchesare due to theknown advantages of using trigenerationthat result in more demand on the energy produced by trigeneration systems[5]. A few papers discussed the utilization of solar energy in trigeneration systems. Reference[6]determined experimentally the performance of a trigeneration system based on a microturbine accompanied by a small solar tower. The study estimated the economicsof using single and double-effect absorption refrigerants. The authors suggested using the

double-effect refrigerant since it exhibited better thermal efficiency and lower operatingcostsas compared to the single-effect absorption refrigerant.Reference [7]examined the monthly primary energy consumption and the forecast monthly CO_2 emission of four systems. Two systems were trigeneration systems which one of them was based on a phosphoric acid fuel cell(PAFC) and the other was based on a solar thermal cycle.The other two systems were a plant with integrated photovoltaic solar cells and a conventional system with electricity from a grid. They observed thatthe system with the PAFC showed constant pollution reduction whereas the system operatingwith the solar thermal cyclehaddesirable pollution reduction in summer. On theother side, the solar thermal cyclehad the most energy saving.Medrano et al. [8]investigated a trigeneration system using thermal collectors to support the production of heating and cooling, and an internal combustion engine as a prime mover. A significant saving in energy and also reduction in CO_2emission wereobtainedas results of the study.

Reference[9] introduced a 100 MW cogeneration system with a central receiver cycle and conducted thermodynamic analysis, preliminary cost estimates and unit energy cost evaluations. Reference [10] studied a $100kW_e/700kW^{th}$ distributed receiver; solar-thermal power plant, which was installed in desert location southwest of Kuwait, designed to supply the fresh water andelectricity, requirements of an agricultural desert settlement. For a solar cogeneration system, reference [11]determined the optimal-value ofoverall effective utilization factor (EUF);then, primary performance parametersof the cycle were investigated at optimum operation.Reference [12] examined the performance and cost of a concentrating photovoltaic/thermal (CPVT) system with single effect absorption refrigeration and the results exhibited that the combined solar power and cooling generation system can be comparable to, and sometimes better than, the conventional system under a wide range of economic conditions.Reference [13] proposed a focusing collector-driven, an irreversible Carnot cogeneration system for air conditioning and refrigeration.The optimal performance of the system was then conducted by using the energetic optimization method. Also, In order to overcome the internal irreversibilities for the system start-up, a minimum value of total solar irradiation required wasdetermined and the influence of the collector design parameters on that value was studied. A new approach to describe the long-term performance of general solar thermal cycles, was presented by reference [14], based on the computation of two important values, related to the maximum and minimum temperature levels that regard the load and, subsequently, examples for solar cogeneration systems were illustrated. For the purpose of numerical modeling of a cogeneration system including a solar collector, a thermal storage reservoir, a hot water heat exchanger, a gas burner and an absorption cooling cycle, a mathematical code that combines empirical and fundamental correlations, and principles of thermodynamics, heat and mass transfers, was developed by Vargas et al. [15]. So transient and steady state responses of the system, under various design and operating conditions were simulated.Reference [16] generated a simulation computercode to identify the thermodynamic performance of concentrating solar cogeneration power plants (CSCPP) and therefore, effects of the most important design parameters on the efficiency of integrated gas turbine solar cogeneration power plant (IGSCP) were investigated. In another study,reference[17] carried outthe exergetic analysis of a solar-driven trigeneration system consideringa single effect absorption refrigerant cycle, an organic Rankine cycle (ORC) and a set of parabolic trough collectors (PTCs) for the system.

In this study a mathematical modeling is carried out by the codes developed inMATLAB software in order to estimate PTCsoptical efficiency based on the sun irradiation during the day, a thermodynamic modeling is then conducted to evaluate the thermodynamic properties of the operating fluid (water) moving through the receiver tube of the collectors. The operating fluid transfers heat into the sub-cycles in order to generate electricity and refrigeration power. Alsoa heat recovery cycle is considered to produce domestic hot water (DHW) fromexhaust gases of the auxiliary unit. Exergy and exergoeconomic analyses are then carried out based on solar irradiation at noontime of a specified day. Finally a parametric study and multi objective optimization by using genetic algorithmare performed in order to improve system performance.The novelties of this work are: theoptimization of the PTCs length by dynamic modeling of the solar field during the day to achieve the best design of the solar field appropriate to the corresponding sub-cycles;modeling of solar irradiation during the day based on the studied region, Bushehr, conditions instead of considering a mean value of radiation during a year;using a cascade ORC(instead of a single ORC) asmain power generation subsystemto increase the energy efficiency of the whole system;power producing in absorption chillersubsystem by an ammonia turbineplaced after the Generator in order to supply some part of internal required power of the system such as the pumps power and etc; Additionally, this paper presents a number of analyses (energy, exergy, exergoeconomic, multi-criteria optimization) which are not simultaneously included in the previous papers available in literature;Besides, the mentioned analyses are investigated by adynamic (live) link implementation between MATLAB and EES (Engineering Equation Solver) during the modeling.ItenabledMATLAB software to solve the system of equations in which the thermodynamic properties of materialswas required, by numerical methodsin the shortest time.

It is expected that the results of present study are useful for power and solar industries as a significant amounts of electrical and cooling powers are produced from the renewable sourcesfor the purpose of reducing GHG and air pollutantsemissions in the world.

2. System Description

A scheme of the proposed trigeneration system is shown in Fig. 1which uses two energy sources, solar energy from the sun is collected by the Solar Field that consists of 8 parallel rows of series PTCs and natural gas combustion in anauxiliary unit, Aux. The main outputs of the system are electric power, cooling capacity and domestic hot water.

The whole system is divided into three subsystems that are integrated to a main cycle as follows:

2.1 Main cycle (I):

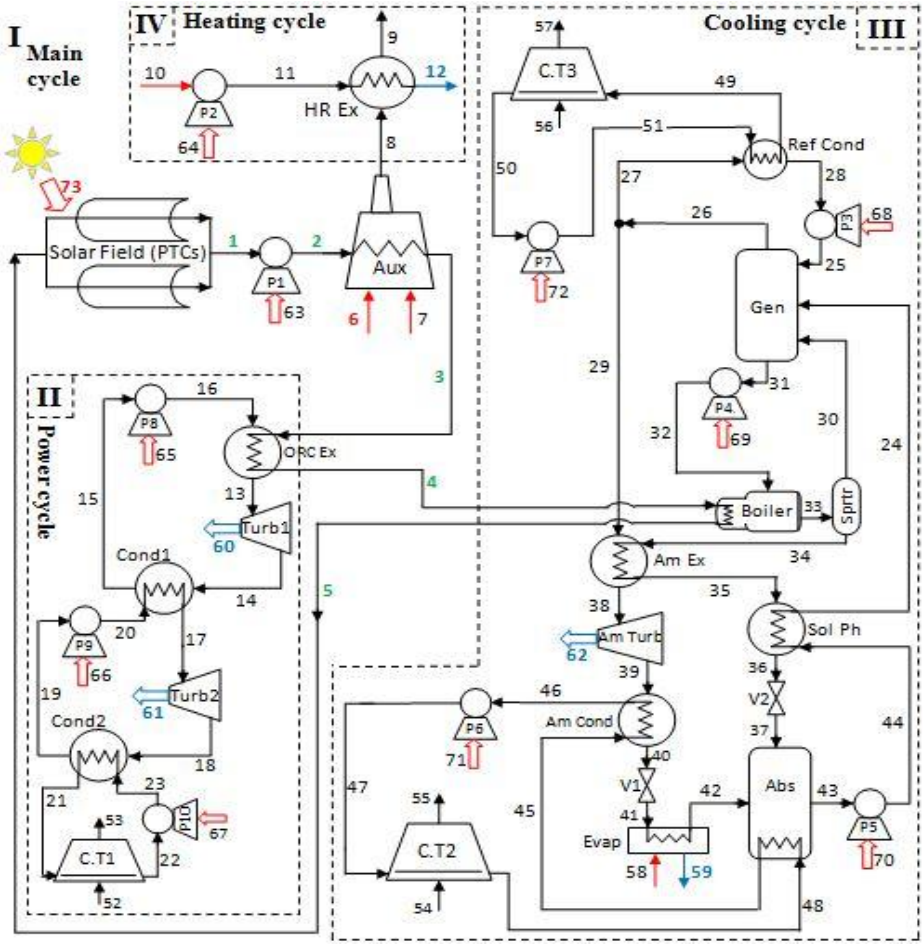

Fig. 1. Solar driven trigeneration system

This main cycle is in charge of providing energy for whole system so that the PTCs absorb the solar energy and transfer the part of the useful heat to the operating fluid moving through receiver tube of collectors. Stream 7 supplies Aux with fresh air, where it is mixed with natural gas and, consequently, the mixture is burnt to produce steam with a quality of 0.3 from saturated liquid water provided by PTCs at maximum irradiation conditions. A lower amount of sun irradiation result in a higher amount of fuel consumption by the Aux as a steady state conditions at the Aux output, stream 3, are obtained during the day (at a temperature of 213.4 °C). The PTCs consist of a metal tube named receiver tube that is coated by a black absorber selective material (named Coating) in order to absorb more irradiation. As mentioned above, water is selected as absorbing medium inside the collectors because of its high value of heat capacity, low temperature required for bottoming cycle and its availability in the proposed region. For the purpose of reducing heat loss due to the free convection effects, the receiver tube is covered by a glass named Glass cover as the annulus space gas is evacuated. The solar radiations reflect and concentrate to the receiver tube after passing the glass cover by the parabola reflectors around the receiver. The PTCs are equipped with a sun tracker with East-West tracking about a horizontal North-South axis for the optical efficiency increment. Finally, the main operating fluid (i.e. water) returns to the solar filed, PTCs, at a temperature of 101 °C (stream 5), after heat transferring to the considered subsystems.

2.2 Power cycle (II):

Provided steam from Main cycle(I)enterssubsystem II, which is thepower cycle, in theORC Ex to produce superheated R600a (at a temperature of 206.5 °C and pressure of 102 bar) that is the operating fluid of the cascade ORC. The resulting R600a is expanded inTurb1 to produce electrical power. The residual heat is converted to electrical power inTurb2 and the exhaust R600a passes through the Cond2 in order to complete the power cycle. A cascade scheme of ORC exhibits a higher value of energy efficiency than a simple one due to the heat recovered from the Cond1 condenser.

2.3 Cooling cycle (III):

The condensed steam coming out of ORC Ex (i.e. stream4) is sent to Boiler at a temperature of 165 °C toevaporate NH_3/H_2O solution. The vapor phase of mentioned solution is separated by the Sprtrand is used in the

Gen (as distillation column) of the absorptionrefrigerationcycle. The refrigerant (NH_3) is separated from NH_3/H_2O vapor in the Gendue to the heat made by the Boiler and mass transfer between the liquid and vapor phases of solution on the trays. After refrigerant has reached the desired purity (about 100%) in the Gen, it is expanded to stream39 by the AmTurband, so, with a lower pressure and temperature and enters the Am Cond in order to releaseits heat to the ambient by the cooling towercomponent, C.T2. The condensed NH_3 passes through an expansion valve, V1, andthen the Evapand after absorbing the heat and producing cold air (stream 59, 61.3 kg/s and 11 °C), it is vaporized and enters the Abs, where it is mixed with the lean mixture of NH_3/H_2O which comes from theSprtr through anAm Exand solution preheater, Sol Ph,and is converted to a rich mixture of NH_3/H_2O. Then the mixture from the Abs is pumped into the Gen through theSol Phin order to preheating.The mixture is set to enter the Gen at a temperature of 70 °C and a pressure of 22 bars with a flow rate of 2.2 kg/s as design parameters (stream 24). A reflux stream is separated from stream26 and is returned to the Gen (at a saturated liquid state) after condensing in Ref Condin order to improvethe purity of produced NH_3. A heat removal is needed in the Abs to enhance the efficiency of absorption exothermic process. Also the AmExreheats the NH_3 before entering the AmTurb by the high temperature lean mixture. Finally the cold air generated can be used for the purpose of air conditioning.

2.4 Heating cycle (IV):

In the subsystem IV, high temperature (501.2 °C) stack gases from Aux are utilized to meet the heating demand by producing 70 °C domestic hot water (i.e. stream 12) from water at environment conditions (i.e. stream 10) through aheat recovery heat exchanger, HR Ex. The combustion products leave the cycle and enter the environment at a low temperature of 72°C (stream 9).

3. Materials and Methods

The solar and thermodynamic modeling of the proposed solar trigeneration system is described in this section. The thermodynamic properties, exergy of the streams and exergoeconomic analysisare determined by solving energy, exergy and cost balances equations via the codes developed in MATLAB software.The MATLAB is linked to the EES software in order to receive thermodynamic properties of different fluids inside the try and error loops[18]. Also the sun radiation and the absorbed irradiation by the collector's fluid in the Solar Field are calculated at any time of day as the code is running.

For simplifying the theoretical analysis of the system, following assumptions are considered:

- There are no pressure drops through pipes except to the receiver tube of PTCs.
- There is no heat generation in the receiver tube and the solar radiation is considered as a constant heat flux term in energy balance equations in each time step.
- All of the flows are fully developed.
- The sky and the glass cover on the receiver tube are assumed to act like a gray body and a black body in the radiation heat transfer calculations respectively.
- A two dimensional heat transferring is considered for the PTCs modeling (radius and axis dimensions).
- Changes in potential and kinetic exergies are neglected.
- The turbines and heat exchangers are assumed to be adiabatic.
- All of the devices except the Solar Field, P1, Aux, P2 and HR Ex operate at steady conditions.

3.1 Solar Analysis

For solar calculations, three steps are considered: 1.Calculating the amount of the solar radiation that arrives to the solar field from the extraterrestrial, 2.Obtaining the optical efficiency of the collectors and 3.Applying the mass and energy balance principles to the receiver tube to calculate the amount of fluid temperature increment during its moving through the receiver tube.

For this purpose the incidence angle or θ,whichis defined as the angle between sun's rays and the normalon a surface,is determined by the mathematical expression below that is derived by considering the operation of the sun tracker which pivots the PTCs about a horizontal North-South axis in order to minimize the incidence angle and maximize the absorbed radiationinto the receiver tube[19]:

$$\cos(\theta) = \sin(\alpha) \times \cos(h_a) + \cos(\delta) \times \sin^2(h_a) \quad (1)$$

Where the altitude angle (α), the hour angle (h_a) and the declination angle (δ) are functions of the time of day, the day of year and the latitude and longitude of where the solar field is located. More detail description is provided by [19].

So the amount of the solar radiation that arrives to the surface of PTCs will be equal to:

$$Q_{sol} = Irr \times A_{col} \times \cos(\theta) \quad (2)$$

Where the solar irradiation term (*Irr*, kW/m^2)is measured by Pyranometer equipment located in the studied region.

The optical efficiency of the PTCs (η_{opt}) presents the share of the Q_{sol} that is reflected and received by the glass cover andreceiver tube. Opticalefficiency of a PTC depends on the size of the receiver, the surface angle errors of the parabolic mirrorand solar beam spread. According to [20] these errors or imperfections are of two types, namely random and non-random. Random errors are modeled statistically, by total reflectedenergy distribution standard deviations at normal incidence. Non random errors are determined by the misalignment angle error and the displacement of the receiver from the focus of the parabola i.e. receiver dislocation distance[21].

So it is usually difficult to estimate the optical efficiency. In this work, a correction factor (Ω) is carried out based on a

research in 2003 that determined the value of each mentioned errors and other effective parameters on the optical efficiency[22]. Therefore theoptical efficiency relation can be expressed as below:

$$\eta_{opt} = \rho_{cl} \times \Omega \quad (3)$$

So the heat absorbedby the glass cover is:

$$Q_g = Q_{sol} \times \eta_{opt} \times \alpha_{a,g} \quad (4)$$

And the heat accepted by receiver tube will be:

$$Q_c = Q_{sol} \times \eta_{opt} \times \tau_g \times \alpha_{a,c} \quad (5)$$

Some information about the glass cover and absorbent coating properties aredemonstrated in Table 1.

3.2 Energy Analysis

The conservation laws of mass, momentum, energy and their corresponding assumptions are used for the purpose of system analyzing. Each component inthe system can be treated as a control volume. For a control volume with inlet *i*and outlet*o*, mass and energy conservation are as below[23]:

$$\sum \dot{m}_i = \sum \dot{m}_o \quad (6)$$

$$\sum Q - \sum \dot{W} = \sum \dot{m}_o h_o - \sum \dot{m}_i h_i \quad (7)$$

As shown in Fig. 1, entering liquid water to the PTCs (i.e. stream 5) absorbs the solar radiation and heats up. The control volume (C.V) considered for applying the principle of energy balance to the PTCs is shown in Fig.2.

The sun radiates to the reflectors of the PTCs and the glass cover receivesQ_g and the outer surface of the receiver tube receives Q_c. Then Q_c is transferred to the working fluid, water, by $Q_{cnd,c}$ (conduction heat transfer due to the thickness of the metal tube), and then by $Q_{cnv,fl}$ (forced convection heat transfer from inner surface of tube to the fluid beside it). The $Q_{cnv,fl}$ causes $Q_{i,fl}$ (inlet energy of the fluid to the C.V) converts to the $Q_{o,fl}$ (outlet energy of the fluid) and an incrementof temperature is achieved. Convection ($Q_{cnv,c}$) and radiation ($Q_{rad,c}$) heat transfers between tube and glass occurs because of temperature difference between outer surface of tube and inner surface of glass. The annulus space between them is filled with air at a vacuum condition in order to reduce heat loss from the outer surface of the receiver tube. Finally the heat loss from the glass cover is due to the conduction ($Q_{cnd,g}$), radiation ($Q_{rad,g}$) and free convection ($Q_{cnv,g}$) heat transfers.

Energy balance equations are used to obtain unknown

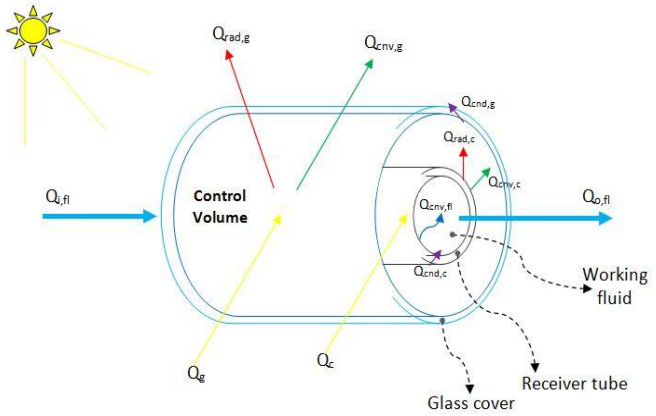

temperature of each surface. The main energy balance equation for the mentioned C.V is written as follows.

$$Q_g + Q_c = Q_{cnv,g} + Q_{rad,g} + (Q_{o,fl} - Q_{i,fl}) \quad (8)$$

Newton's law of cooling provides the equation for the

Fig. 2. The control volume of the PTCs

convection heat transfer calculation in acylindricalcoordinates as follows[24]:

$$Q_{cnv,fl} = h_{cnv} \times 2 \times r_i \times \pi \times (T_i - T_m) \times L_l \quad (9)$$

The relation for radiation heat transfer between twoconcentric cylinders is[24]:

$$Q_{rad,c} = \frac{\sigma \times 2 \times r_{o,ic} \times \pi \times \left({T_{o,ic}}^4 - {T_{i,oc}}^4\right) \times L_l}{\frac{1}{\varepsilon_{e,i}} + \frac{(1-\varepsilon_{e,o}) \times r_{o,ic}}{\varepsilon_{e,o} \times r_{i,oc}}} \quad (10)$$

And the relation for radiation heat transfer between a cylinders and the sky is[24]:

$$Q_{rad,g} = \sigma \times 2 \times r_o \times \pi \times \varepsilon_e \times \left({T_o}^4 - {T_{Sky}}^4\right) \times L_l \quad (11)$$

Useful heat gain rate by water in the receiver tube is written as:

$$\Delta Q = Q_{o,fl} - Q_{i,fl} = \dot{m} \times \left(\Delta h + ({V_o}^2 - {V_i}^2)/2\right) \quad (12)$$

Where the velocity is calculated from the below equation[25]:

$$V = \dot{m}/(\rho \times \pi \times {r_i}^2) \quad (13)$$

For the pressure drop calculations, the expression below is useful[25]:

$$\Delta P = f_f \times L_l \times (\rho \times V^2)/(4 \times r_i) \quad (14)$$

Where, f_f is the friction factorobtained from Moody

Table 1. Glass cover and absorbent coating materials and properties

	material	Transmittance coefficient	Absorptance coefficient	Emissivity coefficient
Absorbent coating	Solel UVAC Cermentavg	-	0.955	*
Glass cover	Pyrex glass	0.965	0.02	0.86
* A function of temperature [22]				

diagram.

All of the other needed heat transfer equations and convection heat transfer coefficients can be computed from their proper equations expressed in the reference books.

Energy efficiency of the trigeneration system isdetermined as follows:

$$\eta_{total} = \frac{\dot{W}_{Net} + \dot{W}_{Ref} + \dot{W}_{DHW}}{LHV \times \dot{m}_f + Q_{sol}} \quad (15)$$

$\dot{W}_{Net}$, $\dot{W}_{Ref}$ and $\dot{W}_{DHW}$ are the three products of system i.e. the net electric, cooling and heating power produced respectively. Also LHV (Low Heating Value) of the fuel (CH_4) is considered to be about 50034.78 kJ per kg of fuel consumed[26].

3.3 Exergy Analysis

Exergy is the maximum work that can be obtained from a given form of energy using the environmental parameters as the reference state [27]. In the other words, it is an attribute of the system and environment together. Generally the exergy,$\dot{X}$,of a substance is oftendivided into four components; Two common ones are physical exergy, $\dot{X}_{PH}$, andchemical exergy,$\dot{X}_{CH}$, which are indicated as follows [28]:

$$\dot{X}_{PH} = \dot{m} \times [(h - h_0) - T_0 \times (s - s_0)] \quad (16)$$

$$\dot{X}_{CH} = \frac{\dot{m}}{MW} \times \left[\sum_{k=1}^{n} y_k \times x_{CH,k} + R \times T_0 \times \sum_{k=1}^{n} y_k \times \ln(y_k)\right] \quad (17)$$

The two others, kinetic exergy ($\dot{X}_{KN}$)and potential exergy ($\dot{X}_{PT}$), areassumed to be negligible here, as speeds are relatively low and elevation changes are small [28]. Physical exergy is defined as the maximum useful work obtainable as a system interacts with an equilibrium state. Chemical exergy is dependent on the chemical composition of the substance at its state and when it is in equilibrium with the reference environment [29].The following exergy balance is obtained by applying the first and the second law of thermodynamics[30]:

$$\dot{X}_Q + \sum_i \dot{m}_i x_i = \sum_o \dot{m}_o x_o + \dot{X}_W + \dot{X}_D \quad (18)$$

$$\dot{X}_Q = (1 - T_0/T) \times Q \quad (19)$$

$$\dot{X}_W = \dot{W} \quad (20)$$

Where $\dot{X}_Q$and$\dot{X}_W$are the corresponding exergies of heat transfer and work which across the boundaries of the control volume. Exergy destruction rate, $\dot{X}_D$, is defined as the difference between fuel and product exergy of a component in which the fuel represents the resources expended to generate the product and the product represents the desired result produced by the system. **Table 2** shows the exergy destruction rate and the exergy efficiency for each component of the system. According to this table, exergy efficiency is defined for each component as the percentage of the fuel exergy provided to the component that is found in the product exergy [28]. The "Dead State" conditions aredetermined as T_0=298 K, P_0=1 bar and an ammonia molar fraction of 0.5 for the NH_3/H_2O solution streams.

The exergy efficiency ofthe whole trigeneration system can be written as:

$$\varepsilon_{total} = \frac{\text{"Whole system product exergy"}}{\text{"Whole system feed exergy"}} = \frac{\dot{X}_{Net} + \dot{X}_{Ref} + \dot{X}_{DHW}}{\dot{X}_f + \dot{X}_{sol}} \quad (21)$$

The "whole system feed exergy" term in the above expression is equal to sum of the exergy of fuel stream to the Aux (stream number 6) as well as the feed exergy to the Solar Field component (i.e. the exergy of solar irradiation, stream number 73). Also the "whole system product exergy" is defined as sum of the net generated electric power plus the generated refrigeration power in terms of exergy (difference between the exergy of streams 59 and 58) plus the amount of hot water generation in terms of exergy (difference between the exergy of streams 12 and 10).

The absorbed sun radiation exergy into the solar collectors is computed fromthe following equation by considering the sun as a black body[31]:

$$\dot{X}_{sol} = Q_{sol} \times \left(1 + (1/3) \times (T_0/T_{Sun})^4 - (4/3) \times (T_0/T_{Sun})\right) \quad (22)$$

T_{Sun} is the sun temperature and is equal to 6000 K [31].

3.4 Exergoeconomic Analysis

For the purpose of exergoeconomic analysis, it is necessary to write the cost balance equation for each component of the system. The cost balance states that the sum of cost rates of all entering exergy streams plus the cost rate associated with the capital investment and operating and maintenance costs ($\dot{Z}$) equals the sum of cost rates associated with all of exiting exergy streams [28]:

$$\dot{C}_Q + \sum_i \dot{C}_i + \dot{Z} = \sum_o \dot{C}_o + \dot{C}_W \quad (23)$$

$$\dot{C} = c \times \dot{X} \quad (24)$$

The average cost per unit exergy of each stream, *c*, is obtained from solving the cost balance equations and appropriate corresponding auxiliary equations simultaneously using the MATLAB software. The auxiliary equations are written based on the principles of Fuel and Product for each component [28]. **Table 3** expresses the cost balances and the corresponding auxiliary equations for each system component. The term$\dot{Z}$ is determined by equipment purchase costs (EPCs) that are calculated from the below equations for each type of equipment. For the pumpswith required power of $\dot{W}_P$ in kW[32]:

Table 2. Exergy destruction rate and exergy efficiency for system components

Component	Exergy destruction rate	Exergy efficiency
C.T 1	$\dot{X}_{D,CT1} = (\dot{X}_{21} - \dot{X}_{22}) - (\dot{X}_{53} - \dot{X}_{52})$	$\varepsilon_{CT1} = (\dot{X}_{53} - \dot{X}_{52})/(\dot{X}_{21} - \dot{X}_{22})$
C.T 2	$\dot{X}_{D,CT2} = (\dot{X}_{47} - \dot{X}_{48}) - (\dot{X}_{55} - \dot{X}_{54})$	$\varepsilon_{CT2} = (\dot{X}_{55} - \dot{X}_{54})/(\dot{X}_{47} - \dot{X}_{48})$
C.T 3	$\dot{X}_{D,CT3} = (\dot{X}_{49} - \dot{X}_{50}) - (\dot{X}_{57} - \dot{X}_{56})$	$\varepsilon_{CT3} = (\dot{X}_{57} - \dot{X}_{56})/(\dot{X}_{49} - \dot{X}_{50})$
P6	$\dot{X}_{D,P6} = (\dot{X}_{71}) - (\dot{X}_{47} - \dot{X}_{46})$	$\varepsilon_{P6} = (\dot{X}_{47} - \dot{X}_{46})/(\dot{X}_{71})$
P5	$\dot{X}_{D,P5} = (\dot{X}_{70}) - (\dot{X}_{44} - \dot{X}_{43})$	$\varepsilon_{P5} = (\dot{X}_{44} - \dot{X}_{43})/(\dot{X}_{70})$
P8	$\dot{X}_{D,P8} = (\dot{X}_{65}) - (\dot{X}_{16} - \dot{X}_{15})$	$\varepsilon_{P8} = (\dot{X}_{16} - \dot{X}_{15})/(\dot{X}_{65})$
P4	$\dot{X}_{D,P4} = (\dot{X}_{69}) - (\dot{X}_{32} - \dot{X}_{31})$	$\varepsilon_{P4} = (\dot{X}_{32} - \dot{X}_{31})/(\dot{X}_{69})$
P9	$\dot{X}_{D,P9} = (\dot{X}_{66}) - (\dot{X}_{20} - \dot{X}_{19})$	$\varepsilon_{P9} = (\dot{X}_{20} - \dot{X}_{19})/(\dot{X}_{66})$
P10	$\dot{X}_{D,P10} = (\dot{X}_{67}) - (\dot{X}_{23} - \dot{X}_{22})$	$\varepsilon_{P10} = (\dot{X}_{23} - \dot{X}_{22})/(\dot{X}_{67})$
P3	$\dot{X}_{D,P3} = (\dot{X}_{68}) - (\dot{X}_{25} - \dot{X}_{28})$	$\varepsilon_{P3} = (\dot{X}_{25} - \dot{X}_{28})/(\dot{X}_{68})$
P2	$\dot{X}_{D,P2} = (\dot{X}_{64}) - (\dot{X}_{11} - \dot{X}_{10})$	$\varepsilon_{P2} = (\dot{X}_{11} - \dot{X}_{10})/(\dot{X}_{64})$
P7	$\dot{X}_{D,P7} = (\dot{X}_{72}) - (\dot{X}_{51} - \dot{X}_{50})$	$\varepsilon_{P7} = (\dot{X}_{51} - \dot{X}_{50})/(\dot{X}_{72})$
P1	$\dot{X}_{D,P1} = (\dot{X}_{63}) - (\dot{X}_{2} - \dot{X}_{1})$	$\varepsilon_{P1} = (\dot{X}_{2} - \dot{X}_{1})/(\dot{X}_{63})$
V2	$\dot{X}_{D,V2} = (\dot{X}_{36} - \dot{X}_{37})$	-
V1	$\dot{X}_{D,V1} = (\dot{X}_{40} - \dot{X}_{41})$	-
Evap	$\dot{X}_{D,Evap} = (\dot{X}_{41} - \dot{X}_{42}) - (\dot{X}_{59} - \dot{X}_{58})$	$\varepsilon_{Evap} = (\dot{X}_{59} - \dot{X}_{58})/(\dot{X}_{41} - \dot{X}_{42})$
Sol Ph	$\dot{X}_{D,Sol\ Ph} = (\dot{X}_{35} - \dot{X}_{36}) - (\dot{X}_{24} - \dot{X}_{44})$	$\varepsilon_{Sol\ Ph} = (\dot{X}_{24} - \dot{X}_{44})/(\dot{X}_{35} - \dot{X}_{36})$
Am Ex	$\dot{X}_{D,Am\ Ex} = (\dot{X}_{34} - \dot{X}_{35}) - (\dot{X}_{38} - \dot{X}_{29})$	$\varepsilon_{Am\ Ex} = (\dot{X}_{38} - \dot{X}_{29})/(\dot{X}_{34} - \dot{X}_{35})$
ORC Ex	$\dot{X}_{D,ORC\ Ex} = (\dot{X}_{3} - \dot{X}_{4}) - (\dot{X}_{13} - \dot{X}_{16})$	$\varepsilon_{ORC\ Ex} = (\dot{X}_{13} - \dot{X}_{16})/(\dot{X}_{3} - \dot{X}_{4})$
Boiler	$\dot{X}_{D,Boiler} = (\dot{X}_{4} - \dot{X}_{5}) - (\dot{X}_{33} - \dot{X}_{32})$	$\varepsilon_{Boiler} = (\dot{X}_{33} - \dot{X}_{32})/(\dot{X}_{4} - \dot{X}_{5})$
Cond1	$\dot{X}_{D,Cond1} = (\dot{X}_{14} - \dot{X}_{15}) - (\dot{X}_{17} - \dot{X}_{20})$	$\varepsilon_{Cond1} = (\dot{X}_{17} - \dot{X}_{20})/(\dot{X}_{14} - \dot{X}_{15})$
Cond2	$\dot{X}_{D,Cond2} = (\dot{X}_{18} - \dot{X}_{19}) - (\dot{X}_{21} - \dot{X}_{23})$	$\varepsilon_{Cond2} = (\dot{X}_{21} - \dot{X}_{23})/(\dot{X}_{18} - \dot{X}_{19})$
HR Ex	$\dot{X}_{D,HR\ Ex} = (\dot{X}_{8} - \dot{X}_{9}) - (\dot{X}_{12} - \dot{X}_{11})$	$\varepsilon_{HR\ Ex} = (\dot{X}_{12} - \dot{X}_{11})/(\dot{X}_{8} - \dot{X}_{9})$
Ref Cond	$\dot{X}_{D,Ref\ Cond} = (\dot{X}_{27} - \dot{X}_{28}) - (\dot{X}_{49} - \dot{X}_{51})$	$\varepsilon_{Ref\ Cond} = (\dot{X}_{49} - \dot{X}_{51})/(\dot{X}_{27} - \dot{X}_{28})$
Am Cond	$\dot{X}_{D,Am\ Cond} = (\dot{X}_{39} - \dot{X}_{40}) - (\dot{X}_{46} - \dot{X}_{45})$	$\varepsilon_{Am\ Cond} = (\dot{X}_{46} - \dot{X}_{45})/(\dot{X}_{39} - \dot{X}_{40})$
Abs	$\dot{X}_{D,Abs} = (\dot{X}_{37} + \dot{X}_{42} - \dot{X}_{43}) - (\dot{X}_{45} - \dot{X}_{48})$	$\varepsilon_{Abs} = (\dot{X}_{45} - \dot{X}_{48})/(\dot{X}_{37} + \dot{X}_{42} - \dot{X}_{43})$
Am Turb	$\dot{X}_{D,Am\ Turb} = (\dot{X}_{38} - \dot{X}_{39}) - \dot{X}_{62}$	$\varepsilon_{Am\ Turb} = \dot{X}_{62}/(\dot{X}_{38} - \dot{X}_{39})$
Turb1	$\dot{X}_{D,Turb1} = (\dot{X}_{13} - \dot{X}_{14}) - \dot{X}_{60}$	$\varepsilon_{Turb1} = \dot{X}_{60}/(\dot{X}_{13} - \dot{X}_{14})$
Turb2	$\dot{X}_{D,Turb2} = (\dot{X}_{17} - \dot{X}_{18}) - \dot{X}_{61}$	$\varepsilon_{Turb2} = \dot{X}_{61}/(\dot{X}_{17} - \dot{X}_{18})$
Sprtr	$\dot{X}_{D,Sprtr} = \dot{X}_{33} - (\dot{X}_{30} + \dot{X}_{34})$	$\varepsilon_{Sprtr} = (\dot{X}_{30} + \dot{X}_{34})/\dot{X}_{33}$
Gen	$\dot{X}_{D,Gen} = \dot{X}_{24} - \left((\dot{X}_{26} - \dot{X}_{25}) + (\dot{X}_{31} - \dot{X}_{30})\right)$	$\varepsilon_{Gen} = \left((\dot{X}_{26} - \dot{X}_{25}) + (\dot{X}_{31} - \dot{X}_{30})\right)/\dot{X}_{24}$
Aux	$\dot{X}_{D,CC} = (\dot{X}_{6} + \dot{X}_{7} - \dot{X}_{8}) - (\dot{X}_{3} - \dot{X}_{2})$	$\varepsilon_{CC} = (\dot{X}_{3} - \dot{X}_{2})/(\dot{X}_{6} + \dot{X}_{7} - \dot{X}_{8})$
Black Point	$\dot{X}_{D,RD} = \dot{X}_{26} - (\dot{X}_{27} + \dot{X}_{29})$	$\varepsilon_{RD} = (\dot{X}_{27} + \dot{X}_{29})/\dot{X}_{26}$
Solar Field	$\dot{X}_{D,SF} = \dot{X}_{73} - (\dot{X}_{1} - \dot{X}_{5})$	$\varepsilon_{SF} = (\dot{X}_{1} - \dot{X}_{5})/\dot{X}_{73}$

$$EPC_P = 3540 \times \dot{W}_P^{\ 0.71} \quad (25)$$

And for the heat exchangers with heat transfer area of A_{HE} in unit of m^2[32]:

$$EPC_{HE} = 130 \times (A_{HE}/0.093)^{0.78} \quad (26)$$

For other types of equipments, the purchase cost is observed form Ref. [33]. Particularly the cost of PTCs is estimated to be about 180.5 \$/m^2. So $\dot{Z}$ is carried out for each component from expression as follows[34]:

$$\dot{Z} = (EPC \times CRF \times \gamma)/(\omega \times 3600) \quad (27)$$

Where the capital recovery factor (*CRF*), the maintenance factor, γ, and the number of systemoperating hours in a year are considered to be 15%, 1.06 and 8000 hr respectively.

There are various parameters that play significant roles in the exergoeconomic analysis such as: the average cost per unit exergy of fuel (c_F), the average cost per unit exergy of product (c_p), the cost flow rate associated with the exergy destruction ($\dot{C}_D$), the exergoeconomic factor (*f*) and the relative cost difference (r_r)which are explained as follows[28]:

$$c_F = \dot{C}_F/\dot{X}_F \quad (28)$$

$$c_p = \dot{C}_p/\dot{X}_p \quad (29)$$

$$\dot{C}_D = c_F \times \dot{X}_D \quad (30)$$

$$f = \dot{Z}/(\dot{Z} + c_F \times (\dot{X}_D + \dot{X}_{Loss})) \quad (31)$$

$$r_r = (c_p - c_F)/c_F \quad (32)$$

The exergoeconomic factor in equation (31) is a parameter which expresses the relative importance of a component cost to the cost of exergy destruction and loss associated with that component. Because of the adiabatic assumption, exergy loss($\dot{X}_{Loss}$) is considered to be negligible for various

Table 3. Cost balances and corresponding auxiliary equations for system components

Component	Cost rate balance equation	Auxiliary equations
C.T 1	$\dot{Z}_{CT1} + (\dot{C}_{21} - \dot{C}_{22}) = (\dot{C}_{53} - \dot{C}_{52})$	$c_{21} = c_{22}$
		$c_{52} = 0$
C.T 2	$\dot{Z}_{CT2} + (\dot{C}_{47} - \dot{C}_{48}) = (\dot{C}_{55} - \dot{C}_{54})$	$c_{47} = c_{48}$
		$c_{54} = 0$
C.T 3	$\dot{Z}_{CT3} + (\dot{C}_{49} - \dot{C}_{50}) = (\dot{C}_{57} - \dot{C}_{56})$	$c_{49} = c_{50}$
		$c_{56} = 0$
P6	$\dot{Z}_{P6} + (\dot{C}_{71}) = (\dot{C}_{47} - \dot{C}_{46})$	$c_{71} = c_{62}$
P5	$\dot{Z}_{P5} + (\dot{C}_{70}) = (\dot{C}_{44} - \dot{C}_{43})$	$c_{70} = c_{62}$
P8	$\dot{Z}_{P8} + (\dot{C}_{65}) = (\dot{C}_{16} - \dot{C}_{15})$	$c_{65} = c_{60}$
P4	$\dot{Z}_{P4} + (\dot{C}_{69}) = (\dot{C}_{32} - \dot{C}_{31})$	$c_{69} = c_{62}$
P9	$\dot{Z}_{P9} + (\dot{C}_{66}) = (\dot{C}_{20} - \dot{C}_{19})$	$c_{66} = c_{61}$
P10	$\dot{Z}_{P10} + (\dot{C}_{67}) = (\dot{C}_{23} - \dot{C}_{22})$	$c_{67} = c_{61}$
P3	$\dot{Z}_{P3} + (\dot{C}_{68}) = (\dot{C}_{25} - \dot{C}_{28})$	$c_{68} = c_{62}$
P2	$\dot{Z}_{P2} + (\dot{C}_{64}) = (\dot{C}_{11} - \dot{C}_{10})$	$c_{64} = c_{60}$
		$c_{10} = 0$
P7	$\dot{Z}_{P7} + (\dot{C}_{72}) = (\dot{C}_{51} - \dot{C}_{50})$	$c_{72} = c_{62}$
P1	$\dot{Z}_{P1} + (\dot{C}_{63}) = (\dot{C}_{2} - \dot{C}_{1})$	$c_{63} = c_{60}$
V2	$\dot{Z}_{V2} + \dot{C}_{36} = \dot{C}_{37}$	None
V1	$\dot{Z}_{V1} + \dot{C}_{40} = \dot{C}_{41}$	None
Evap	$\dot{Z}_{Evap} + (\dot{C}_{41} - \dot{C}_{42}) = (\dot{C}_{59} - \dot{C}_{58})$	$c_{41} = c_{42}$
		$c_{58} = 0$
Sol Ph	$\dot{Z}_{Sol\ Ph} + (\dot{C}_{35} - \dot{C}_{36}) = (\dot{C}_{24} - \dot{C}_{44})$	$c_{35} = c_{36}$
Am Ex	$\dot{Z}_{Am\ Ex} + (\dot{C}_{34} - \dot{C}_{35}) = (\dot{C}_{38} - \dot{C}_{29})$	$c_{35} = c_{34}$
ORC Ex	$\dot{Z}_{ORC\ Ex} + (\dot{C}_{3} - \dot{C}_{4}) = (\dot{C}_{13} - \dot{C}_{16})$	$c_{3} = c_{4}$
Boiler	$\dot{Z}_{Boiler} + (\dot{C}_{4} - \dot{C}_{5}) = (\dot{C}_{33} - \dot{C}_{32})$	$c_{4} = c_{5}$
Cond1	$\dot{Z}_{Cond1} + (\dot{C}_{14} - \dot{C}_{15}) = (\dot{C}_{17} - \dot{C}_{20})$	$c_{14} = c_{15}$
Cond2	$\dot{Z}_{Cond2} + (\dot{C}_{18} - \dot{C}_{19}) = (\dot{C}_{21} - \dot{C}_{23})$	$c_{18} = c_{19}$
HR Ex	$\dot{Z}_{HR\ Ex} + (\dot{C}_{8} - \dot{C}_{9}) = (\dot{C}_{12} - \dot{C}_{11})$	$c_{8} = c_{9}$
Ref Cond	$\dot{Z}_{Ref\ Cond} + (\dot{C}_{27} - \dot{C}_{28}) = (\dot{C}_{49} - \dot{C}_{51})$	$c_{27} = c_{28}$
Am Cond	$\dot{Z}_{Am\ Cond} + (\dot{C}_{39} - \dot{C}_{40}) = (\dot{C}_{46} - \dot{C}_{45})$	$c_{39} = c_{40}$
Abs	$\dot{Z}_{Abs} + (\dot{C}_{37} + \dot{C}_{42} - \dot{X}_{43}) = (\dot{C}_{45} - \dot{C}_{48})$	$c_{37} = c_{43}$
Am Turb	$\dot{Z}_{Am\ Turb} + (\dot{C}_{38} - \dot{C}_{39}) = \dot{C}_{62}$	$c_{38} = c_{39}$
Turb1	$\dot{Z}_{Turb1} + (\dot{C}_{13} - \dot{C}_{14}) = \dot{C}_{60}$	$c_{13} = c_{14}$
Turb2	$\dot{Z}_{Turb2} + (\dot{C}_{17} - \dot{C}_{18}) = \dot{C}_{61}$	$c_{17} = c_{18}$
Sprtr	$\dot{Z}_{Sprtr} + \dot{C}_{33} = (\dot{C}_{30} + \dot{C}_{34})$	$c_{30} = c_{34}$
Gen	$\dot{Z}_{Gen} + \dot{C}_{24} = (\dot{C}_{26} - \dot{C}_{25}) + (\dot{C}_{31} - \dot{C}_{30})$	$c_{26} = c_{31}$
Aux	$\dot{Z}_{Aux} + (\dot{C}_{6} + \dot{C}_{7} - \dot{C}_{8}) = (\dot{C}_{3} - \dot{C}_{2})$	$c_{8} = 0$
		$c_{6} = 0.00245$
		$c_{7} = 0$
Black Point	$\dot{Z}_{RD} + \dot{C}_{26} = (\dot{C}_{27} + \dot{C}_{29})$	$c_{27} = c_{29}$
Solar Field	$\dot{Z}_{SF} + \dot{C}_{73} = (\dot{C}_{1} - \dot{C}_{5})$	$c_{73} = 0$

components of the system. The parameterr_r indicates the difference between the specific product and fuel cost for each component. This difference is due to the cost rate of exergydestruction and the cost rate associatedwith the investment costs [35].

4. Results and Discussion

4.1 Exergy and Exergoeconomic Analyses

The main energy suppliers of the proposed trigeneration system are PTCs and auxiliary unit, Aux. Since the solar radiation is variable during the day, in the PTCs, water outlet temperature (stream 1) varies and, therefore,Auxis applied for covering this transition. A quasi-dynamic mathematical model considering the transient conditions in the PTCs and other components during the day by small time steps, developed in MATLAB software. The model solves the mass and energy balance equations during the day considering steady state conditions for each time step. This consideration is reasonable due to the slow motion of sun in the sky during the day and, so, the resulted quasi-equilibrium process in the solar collectors thermodynamically.Solar irradiation data is based on the selected region, Bushehr (29 °N, 52 °E), located in Iran on the date 16th of the month August. Bushehr temperature is variable between 14.3 °C and 32.6 °C and maximum and average daily irradiation on a horizontal

surface isalmost0.44 and 0.21 kWh/m^2 during the year respectively.A tracker mode of "E-W tracking about horizontal N-S Axis" is selected for the PTCs operating. Also water,stainless steel (AISI302) and airmaterials are selected as the operating fluid, the receiver tube material and the existence gas in the annular space (the space between receiver tube and glass cover) respectively. By applying the selected PTCs specifications shown in Table 4 and choosing a time step of 15 minutes, the PTCs aredynamically modeled andwater outlet temperature is calculated during the day, considering different PTCs lengths (see Fig.3).

Finally, a length of 150meters for PTCs is selected as the optimum length based on the operating fluid pressure in order to result in saturated liquid water attainment at the maximum radiation in day (to avoid vaporization occurrence in the receiver tube of collectors).As it is observed from Fig.3, the outlet temperature of fluid by the optimum length of PTCs in maximum sun irradiation will be200 °C at 2P.M. The pressure of water in the receiver tube in these conditions is about 19.7bars (absolute) that results in a situation nearthe saturated liquid. The prepared saturated liquid is vaporized in the Aux by 0.3 vapor fraction (2-phase conditions) in order to maximize heat transferring in the ORCEx and, so, net output electric power. A water mass flow rate of7 kg/s is needed in order to produceapproximately 1 MW of net electric power in the ORC cycle; Moreover, forthe purpose of reducing pressure drop of the operating fluid of PTCs, a mass flow rate of 0.875 kg/s is selected for derivation of Fig. 3; Therefore, 8 rows of optimum PTCs length are set in parallel in order to provide desired heat for the operation of whole system.

Since working conditions of the solar collectors are dynamic, a backup energy source is required in order to provide steady amount of outputs as mentioned above. Fig.4 indicates that when amount of solar irradiation in the Solar Field is maximum,CNG (Compressed Natural Gas)consumption by the Aux is minimized; while sum of energy supplying by these two is constant during a day.According to Fig.4, a decrease of 42.3% in fuel (i.e. CNG) consumption of Aux (fuel mass flow rate) is achieved when the solar irradiation goes toward its maximum amount at solar noon. It means that the studied trigeneration system can reduce the fuel consumption about 42.3 percent and its corresponding GHG emissions.

Table 4. Specifications of selected PTCs

Parameter	Value & Unit / Material
Aperture of parabola	5.76 m
Parabola focal distance	2.4 m
PTCs in parallel	8
Outer diameter of glass cover	0.11 m
Thickness of the glass cover	0.006 m
Receiver tube outside diameter	0.055 m
Receiver tube thickness	0.005 m
Annular space pressure	40 kPa (abs)
Reflectivity of the PTCs	0.91
Operating fluid	Water
Material of receiver tube	AISI302
Selective coating type	Solel UVAC Cermentavg
Fluid of annular space	Air
Material of glass cover	Pyrex®

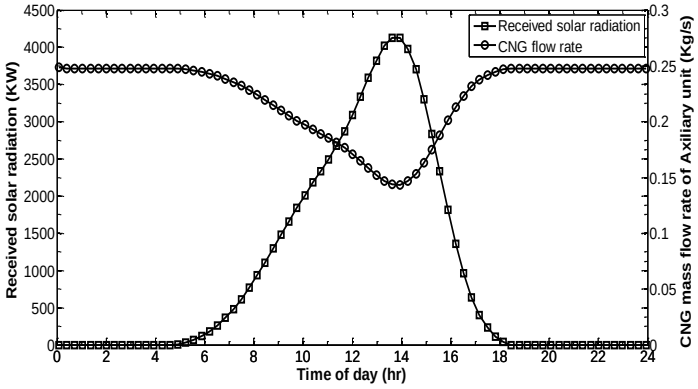

Fig. 4. Variation of received solar radiation by PTCs and corresponding CNG mass flow rate to auxiliary unit, Aux, during the day (16 August)

For the purpose of exergoeconomic analysis of the

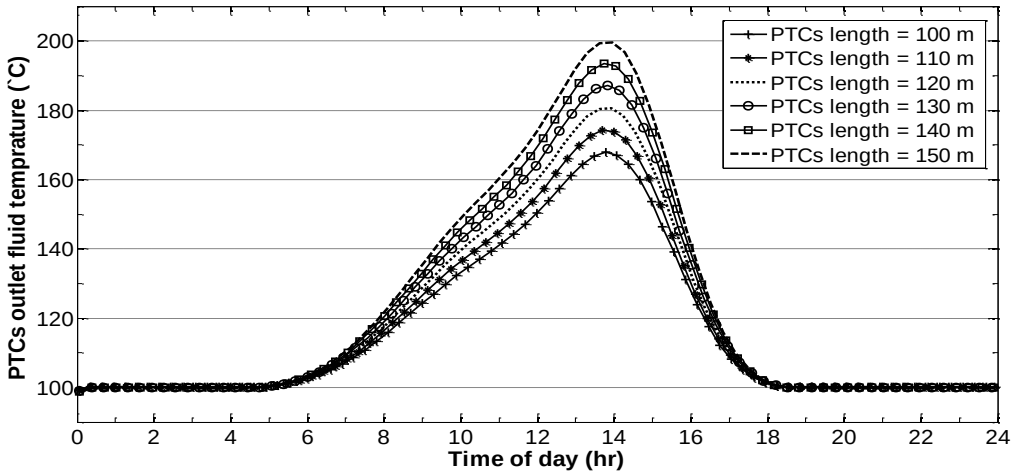

Fig. 3. Variation of water outlet temperature during the day (16th August) for different PTCs lengths

proposed system, a specific time of day, 12 P.M, is selected considering input data shown in Table 5.

Table 5. Input data for thermodynamic modeling

Parameter	Value & Unit
Efficiency of auxiliary unit, Aux	55 %
Excess air percent used in the Aux	200 %
Adiabatic efficiency of the ORC Turb1	75 %
Adiabatic efficiency of the ORC Turb2	75 %
Adiabatic efficiency of the Am Turb	75 %
Inlet pressure of the working fluid to the Aux	20 bar (abs)
Vapor fraction of outlet fluid from the Aux	0.3
Temperature of working fluid, ORC Exoutlet	165 °C
Temperature of working fluid, Boileroutlet	101 °C
Inlet pressure of refrigerator solution to the Gen	22 bar (abs)

The resulted process data of the systemisillustrated in Table 6 for mass streams and Table 7 for energy streams consequently.

The costs of the unknown streams, which are revealed by the solution to the linear system of equations in Table 3, are also listed in Table 8 for mass streams and Table 9 for energy streams of the system.

Table 7. Process streams data (energy streams)

Stream Number	Total Exergy (MW)
60	0.7310
61	0.5973
62	0.0427
63	0.0003
64	0.0041
65	0.2862
66	0.0466
67	0.0022
68	0.00005
69	0.0002
70	0.0085
71	0.0016
72	0.0006
73	2.8785

According toTable 5 and Table 6, the latent heat of vaporization of the main cycle's operating fluid, water, is transferred in the ORC Ex while the Boiler of the cooling cycle receives the sensible heat that remains inthe operating fluid; this is because of priority of electric power generation in such systems rather than the generation of cooling power.The total exergy rate of solar irradiation (stream 73)

Table 6. Process streams data (mass streams)

Stream	Temp. (°C)	Pressure (bar)	Mass flow (kg/s)	Enthalpy (kJ/kg)	Entropy (kJ/kg-K)	Physical Exergy (MW)	Chemical Exergy (MW)	Total Exergy (MW)
1	174.2	19.0	7.000	738.24	2.08	0.85	0.02	0.87
2	174.2	20.0	7.000	738.28	2.08	0.86	0.02	0.87
3	213.4	20.0	7.000	2801.68	6.35	6.40	0.02	6.42
4	165.0	19.9	7.000	698.16	1.99	0.76	0.02	0.78
5	101.0	19.8	7.000	424.69	1.32	0.26	0.02	0.27
6	25.0	4.0	0.171	-3.91	-0.72	0.04	8.79	8.83
7	70.0	4.0	6.435	1302.84	192.27	0.82	0.02	0.85
8	501.2	4.0	6.606	-21423.47	221.49	3.12	0.04	3.16
9	72.0	3.7	6.606	-38864.56	195.00	0.91	0.04	0.95
10	24.0	2.0	15.562	100.75	0.35	0.00	0.04	0.04
11	24.0	4.0	15.562	100.99	0.35	0.00	0.04	0.04
12	70.0	3.9	15.562	293.30	0.95	0.21	0.04	0.24
13	206.5	102.0	12.473	919.25	4.01	2.30	1287.40	1289.70
14	120.7	14.0	12.473	875.11	4.06	1.53	1287.40	1288.93
15	55.0	13.9	12.473	467.43	2.92	0.69	1287.40	1288.09
16	63.7	102.1	12.473	508.07	2.99	0.94	1287.40	1288.34
17	107.5	20.0	11.860	821.58	3.89	1.45	1224.16	1225.61
18	59.9	4.0	11.860	774.35	3.94	0.69	1224.16	1224.86
19	26.0	3.9	11.860	390.89	2.68	0.59	1224.16	1224.76
20	27.4	20.1	11.860	397.30	2.70	0.63	1224.16	1224.79
21	35.7	1.9	83.000	149.48	0.51	0.07	0.21	0.28
22	23.0	1.8	83.000	96.55	0.34	0.01	0.21	0.22
23	23.0	2.0	83.000	96.57	0.34	0.01	0.21	0.22
24	70.0	22.0	2.200	-8844.81	4.60	2.65	25.54	28.20
25	52.0	21.8	0.749	-3790.66	5.20	4.56	14.84	19.40
26	52.4	21.8	1.499	-2698.29	8.55	9.25	29.68	38.93
27	52.4	21.8	0.749	-2698.29	8.55	4.63	14.84	19.47
28	52.0	21.6	0.749	-3790.71	5.20	4.56	14.84	19.40
29	52.4	21.8	0.749	-2698.29	8.55	4.63	14.84	19.47
30	117.8	22.0	1.285	-3147.54	9.08	7.15	24.01	31.16
31	76.3	22.0	2.736	-8151.06	4.79	5.04	34.71	39.75
32	76.3	22.2	2.736	-8151.01	4.79	5.04	34.71	39.75
33	118.0	22.1	2.736	-7399.99	6.84	5.42	34.71	40.13
34	117.8	22.0	1.451	-11167.68	4.86	-1.73	10.71	8.97
35	109.2	21.9	1.451	-11210.95	4.75	-1.75	10.71	8.96
36	41.8	21.8	1.451	-11537.99	3.81	-1.82	10.71	8.89
37	42.2	4.9	1.451	-11537.99	3.82	-1.82	10.71	8.89
38	85.0	21.7	0.749	-2614.53	8.80	4.63	14.84	19.47
39	59.5	15.0	0.749	-2656.10	8.84	4.59	14.84	19.43
40	38.4	15.0	0.749	-3867.54	4.96	4.55	14.84	19.39
41	4.4	5.0	0.749	-3867.54	5.00	4.54	14.84	19.38
42	15.0	4.9	0.749	-2722.62	9.14	4.48	14.84	19.32
43	25.7	4.9	2.200	-9063.58	3.92	2.61	25.54	28.16
44	26.0	22.1	2.200	-9060.46	3.92	2.62	25.54	28.16
45	32.7	2.7	30.000	137.35	0.47	0.02	0.07	0.09
46	39.6	2.6	30.000	165.89	0.57	0.05	0.07	0.12
47	39.6	3.0	30.000	165.94	0.57	0.05	0.07	0.12
48	24.0	2.8	30.000	100.83	0.35	0.01	0.07	0.08
49	33.0	2.9	23.081	138.48	0.48	0.01	0.06	0.07
50	25.0	2.8	23.081	105.01	0.37	0.00	0.06	0.06
51	25.0	3.0	23.081	105.03	0.37	0.00	0.06	0.06
52	24.0	1.0	492.494	297.44	6.86	0.01	0.00	0.01
53	32.0	1.0	492.494	305.49	6.88	0.05	0.00	0.05
54	24.0	1.0	290.973	297.44	6.86	0.01	0.00	0.01
55	30.0	1.0	290.973	303.48	6.88	0.02	0.00	0.02
56	25.0	1.0	86.877	298.45	6.86	0.00	0.00	0.00
57	33.0	1.0	86.877	306.50	6.89	0.01	0.00	0.01
58	25.0	1.0	61.313	298.45	6.86	-0.07	0.00	-0.07
59	11.0	1.0	61.313	284.36	6.82	-0.05	0.00	-0.05

inTable7is obtained from equations (2) and (22) based on the collectors area of 6912 square meters calculated as follows:

$$A_{col} = (B \times L_{tot}) \times Pl \quad (33)$$

Table 8indicates values of 0.88 $/hr and 2.35 $/hr for the cost rates of generated domestic hot water (stream 12) and cooling power (stream 59) respectively. Also high amounts of the cost rates ($\dot{C}$) for some streams in Table 8, are due to the high value of chemical exergy for such streams that affects the total exergy of stream (see equation(24)). Furthermore it can be realized from this table that how favorable the cost rate value of 4.24 $/hr associated with stream 5, increases extremely to the cost rate value of 19.24 $/hr in stream 1 by usingtheSolar Field as a component with free fuel consumption ($\dot{C}_{73} = 0$). Table 9represents values of 59.15 $/hr and62.18 $/hrfor the cost rates of electric power produced by ORC Turb1 and Turb2associated with streams 60 and 61 respectively.

Table 9. Exergy rates, unit exergy costs and cost rates for the energy streams of the system

Stream Number	$\dot{X}$ (MW)	c ($/MJ)	$\dot{C}$ ($/hr)
60	0.731	0.022	59.147
61	0.597	0.029	62.178
62	0.043	0.014	2.133
63	0.000	0.022	0.025
64	0.004	0.022	0.333
65	0.286	0.022	23.161
66	0.047	0.029	4.853
67	0.002	0.029	0.228
68	0.000	0.014	0.002
69	0.000	0.014	0.011
70	0.008	0.014	0.423
71	0.002	0.014	0.080
72	0.001	0.014	0.029
73	2.878	0.000	0.000

Table 8. Exergy rates, unit exergy costs and cost rates for the mass streams of the system

Stream number	$\dot{X}$ (MW)	c ($/MJ)	$\dot{C}$ ($/hr)
1	0.872	0.006	19.236
2	0.873	0.006	19.292
3	6.417	0.004	99.137
4	0.781	0.004	12.064
5	0.274	0.004	4.236
6	8.826	0.002	77.845
7	0.848	0.000	0.000
8	3.160	0.000	0.000
9	0.952	0.000	0.000
10	0.041	0.000	0.000
11	0.044	0.003	0.526
12	0.244	0.001	0.882
13	1289.698	0.020	92055.971
14	1288.932	0.020	92001.300
15	1288.090	0.020	91941.182
16	1288.341	0.020	91968.272
17	1225.614	0.022	95128.822
18	1224.857	0.022	95070.093
19	1224.757	0.022	95062.262
20	1224.792	0.022	95068.199
21	0.279	0.038	38.389
22	0.216	0.038	29.725
23	0.218	0.038	30.077
24	28.199	0.009	890.998
25	19.023	0.009	601.267
26	38.204	0.009	1207.534
27	19.102	0.009	603.769
28	19.023	0.009	601.257
29	19.102	0.009	603.769
30	31.470	0.009	991.403
31	40.413	0.009	1277.355
32	40.413	0.009	1277.391
33	40.837	0.009	1286.253
34	9.364	0.009	294.995
35	9.352	0.009	294.601
36	9.272	0.009	292.101
37	9.268	0.009	292.103
38	19.109	0.009	604.399
39	19.053	0.009	602.627
40	19.015	0.009	601.426
41	19.005	0.009	601.429
42	18.941	0.009	599.398
43	28.158	0.009	887.470
44	28.165	0.009	888.215
45	0.094	0.044	15.005
46	0.124	0.037	16.477
47	0.125	0.037	16.656
48	0.081	0.037	10.739
49	0.068	0.079	19.519
50	0.058	0.079	16.705
51	0.059	0.079	16.784
52	0.011	0.000	0.000
53	0.051	0.050	9.106
54	0.007	0.000	0.000
55	0.018	0.092	6.100
56	0.002	0.000	0.000
57	0.010	0.082	3.075
58	-0.066	0.000	0.000
59	-0.046	-0.014	2.354

The major exergy and exergoeconomic parametersfor various components of the proposed trigeneration system are reported in Table 10.

The summation of $\dot{Z}$ plus $\dot{C}_D$ for each component is also illustrated in Fig. 5 in an ascending order to reveal the components with high value of $\dot{Z} + \dot{C}_D$.

The highest value of $\dot{Z} + \dot{C}_D$ is observed in that Fig. to belong to the ORC Ex, suggesting that attention should be focused on improving this component from the viewpoint of exergoeconomics. The value of 0.94% for the exergoeconomic factor of the ORC Ex based on Table 10 describes that the exergy destruction cost in this component dominates the capital and operating costs; in addition, a low value of exergetic efficiency of 24.07% for this component emphasizes on increasing the exergetic efficiency. Therefore, anincrement in the investment costs for this component is necessary, through increasing its heat transfer area.

The second most significant component in the exergoeconomicanalysis of the studied system is the ORC Turb2 because of its highvalue of $\dot{Z} + \dot{C}_D$. For this component the valueof relative cost difference,r_r, is about 34%. The exergoeconomic factor and exergetic efficiency of the ORC Turb2 are found to be 21.8% and 78.9% respectively. So the exergy and exergoeconomicperformance of this component is satisfactory.However, an improvement

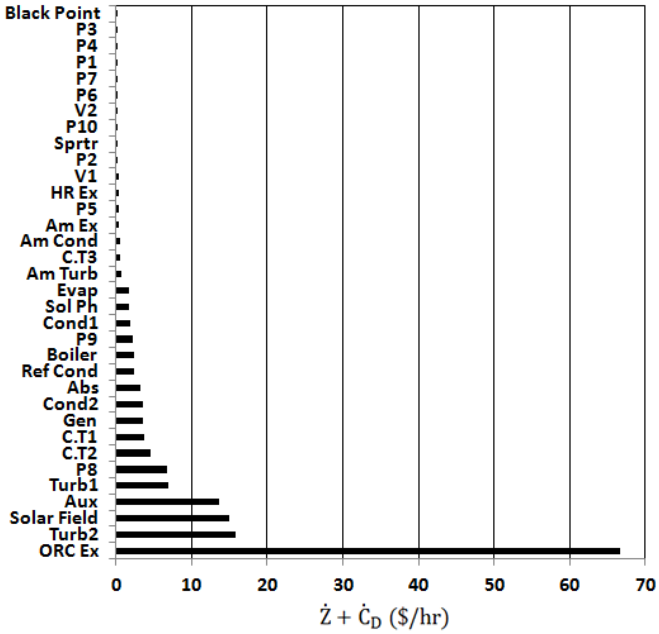

Fig. 5. The value of $\dot{Z}$ plus $\dot{C}_D$ for each component of system

Table 10. The results of exergoeconomic analysis for each component of system

Component	$\dot{X}_{Feed}$ (MW)	$\dot{X}_{Product}$ (MW)	$\dot{X}_D$ (MW)	ε (%)	$\dot{Z}$ ($/hr)	$\dot{C}_D$ ($/hr)	$\dot{Z} + \dot{C}_D$ ($/hr)	r_r (%)	f (%)
C.T 1	0.0630	0.0393	0.0237	62.32	0.442	3.265	3.707	68.66	11.92
C.T 2	0.0444	0.0117	0.0326	26.47	0.182	4.351	4.533	289.46	4.01
C.T 3	0.0099	0.0087	0.0011	88.58	0.260	0.322	0.582	23.33	44.71
P6	0.0016	0.0012	0.0004	75.89	0.099	0.019	0.118	194.41	83.66
P5	0.0085	0.0078	0.0007	91.88	0.322	0.034	0.357	91.84	90.37
P8	0.2862	0.2514	0.0349	87.81	3.929	2.823	6.752	33.20	58.20
P4	0.00023	0.00021	0.00002	91.33	0.024	0.001	0.025	242.48	96.08
P9	0.0466	0.0353	0.0113	75.75	1.083	1.177	2.260	61.49	47.93
P10	0.0022	0.0017	0.0005	75.75	0.124	0.055	0.179	103.49	69.08
P3	0.00005	0.00003	0.00001	76.28	0.008	0.001	0.008	484.92	93.59
P2	0.0041	0.0031	0.0010	75.76	0.193	0.081	0.274	108.62	70.54
P7	0.0006	0.0004	0.0001	75.77	0.050	0.007	0.057	259.75	87.69
P1	0.0003	0.0002	0.0001	79.40	0.031	0.005	0.036	180.61	85.63
V2	9.2722	9.2679	0.0044	99.95	0.002	0.138	0.140	0.05	1.71
V1	19.0146	19.0050	0.0096	99.95	0.003	0.304	0.307	0.05	0.98
Evap	0.0642	0.0205	0.0436	31.99	0.323	1.381	1.704	262.26	18.95
Sol Ph	0.0794	0.0334	0.0459	42.13	0.283	1.447	1.730	164.22	16.36
Am Ex	0.0125	0.0066	0.0060	52.29	0.235	0.188	0.424	205.22	55.55
ORC Ex	5.6365	1.3568	4.2797	24.07	0.625	66.113	66.738	318.40	0.94
Boiler	0.5067	0.4238	0.0829	83.63	1.034	1.281	2.315	35.36	44.65
Cond 1	0.8422	0.8222	0.0200	97.62	0.506	1.429	1.935	3.30	26.14
Cond 2	0.1009	0.0614	0.0395	60.82	0.481	3.069	3.550	74.53	13.55
HR Ex	2.2074	0.2008	2.0066	9.10	0.356	0.000	0.356	-	100.00
Ref Cond	0.0795	0.0094	0.0701	11.85	0.223	2.215	2.438	819.04	9.15
Am Cond	0.0379	0.0299	0.0080	78.85	0.271	0.254	0.525	55.49	51.67
Abs	0.0510	0.0132	0.0378	25.95	0.235	2.985	3.221	307.90	7.31
Am Turb	0.0561	0.0427	0.0134	76.11	0.360	0.423	0.783	58.05	45.94
Turb 1	0.7659	0.7310	0.0350	95.44	4.476	2.495	6.971	13.36	64.21
Turb 2	0.7566	0.5973	0.1593	78.94	3.449	12.366	15.816	34.11	21.81
Sprtr	40.8372	40.8345	0.0027	99.99	0.146	0.085	0.230	0.02	63.19
Gen	28.1989	28.1244	0.0745	99.74	1.222	2.355	3.577	0.40	34.16
Aux	6.5140	5.5447	0.9693	85.12	2.000	11.584	13.584	20.50	14.72
Black Point	38.2042	38.2042	0.0000	100.00	0.004	0.000	0.004	0.00	100.00
Solar Field	2.8785	0.5983	2.2802	20.78	15.000	0.000	15.000	-	100.00

in the exergetic efficiency still can be useful.

The Solar Field has the third highest importance exergoeconomically. The very high value of f for this component proposes that a decrease in capital cost of this component is merited.

On the contrary of the high value of $\dot{Z} + \dot{C}_D$ for the auxiliary unit, Aux, there is low value of r_r and f for this component. Considering a relatively high exergetic efficiency of 85.12%, it can be concluded that the component is operating in an appropriate conditions.

From the viewpoint of exergoeconomics, operating conditions of ORC Turb1are similar to that for the ORC Turb2. However a better value of f and a higher exergetic efficiency of 95.44% for the ORC Turb1, make it more effective exergoeconomically.

For the exergoeconomic analysis of the trigeneration system, C.T2 and C.T1are the next most importance components.Because of the high value of r_r and the low value of f for the C.T2, significant attention should be paid to this component. So, considering the low exergetic efficiency of 26.47%, any investment for the purpose of enhancing the efficiency of C.T2 is remedial. C.T1 has better conditions effectively, because of its lower r_r and higher f. Therefore increase in capital costs of C.T1 is not in priority, although improvement in its efficiency still can improves system performance.

For the component Gen,the value of $\dot{Z} + \dot{C}_D$ equals to3.58$/hr; buta very low value of r_r and a moderate value of f for the key component Gen in cooling cycle, results in a high performance of this component.

The ORC Cond2, Abs and Ref Cond of the cooling cycle also have relatively high values of $\dot{Z} + \dot{C}_D$ among the other components. More attention is need for the Abs and Ref Cond due to their very high value of r_r. The low values of f for the Cond2, Abs and Ref Condsuggest an increasein the heat transfer area for these components. The comparativelyhigher values of exergy destruction in such componentsare mainlydue to the temperature differences between the heat exchanger (condenser) streams.

Changes in the exergoeconomic parameters of the other components do not affect remarkably the exergoeconomic performance of the whole system, as the values of $\dot{Z} + \dot{C}_D$ associated with these components are the lowest in the cycle. Note that the pump P8 has a high value of $\dot{Z} + \dot{C}_D$, but a moderate value of f, a low value of r_r and a high exergetic efficiency of 87.81%; so the relative contribution of this component in thesystem total cost will be low too. The reason of low value of $\dot{Z} + \dot{C}_D$ for the HR Ex in spite of high value of exergy destruction occurred in this component, is the c_8=0 auxiliary equation consideration for the Aux in Table 3. This is because of negligible discharge costs for exhaust gases of Aux (i.e. stream 9) which are vented to the environment at low temperature of 72 °C.

The overall value of the exergoeconomic factor for the solar driven trigeneration system is computed to be23.7%. This expresses that 76.3% of the total system costs are associatedwith the destruction of exergy. Therefore an increasein the capital costs of the components enhances theexergoeconomic performance of the system generally.

Finally Table 11 outlines the output and performance of the whole system. As it is shown in that table, a net electric power of approximately1 MW, cooling capacity of 858 kW and domestic hot water of 15.55 kg/s are generated by the trigeneration system. The following calculations perform energy and exergy efficiencies evaluations by using equations (15) and (21); for energy efficiency calculation:

$$\eta_{\text{total}} = \frac{1008 + 858 + 3173.369}{8559.071 + 3085.165} \times 100 = 43.278\ \%$$

And for exergy efficiency evaluation:

$$\varepsilon_{\text{total}} = \frac{1008 + 20.944 + 203.452}{8825.978 + 2878.459} \times 100 = 10.529\ \%$$

Also the total cost rate of system, $\dot{C}_{total}$, which is the sum of total capital and operating cost rates plus the total exergy destruction cost rate, is determined to be 160 $/hr approximately.

4.2 Parametric Study

A parametric study is done to investigate the effects on the important exergoeconomic parameters of the proposed system of such parametersas inlet temperature of the ORC turbine Turb1, T_{13}, which determine thedegree of superheat; outlet temperature of the ORC Cond1, T_{15}; hot stream outlet temperature of the ORC Ex, T_4 and operating pressure of thede-absorber Gen in the cooling cycle, P_{24}.These parameters include the unit cost of electricity produced by the ORC turbine Turb1, c_{60}, the total exergy destruction cost rate of system,$\dot{C}_{D,total}$, the overallexergoeconomic factor, $f_{overall}$, and the total cost rate of system, $\dot{C}_{total}$.

Fig.6 shows the variations of four significant exergoeconomicparameters withT_{13}.It can be seen in Fig. 6a that as T_{13} increases, c_{60} decreases. This is because of the decrease in $\dot{C}_{60}$and the increase in $\dot{X}_{60}$as T_{13} increases (see Fig. 7 for this reason).The variation of $\dot{C}_{D,total}$with T_{13} is illustrated in Fig. 6b, where it can be observed that $\dot{C}_{D,total}$ is minimized at a particular value of T_{13} mainly due to a

Table 11. Performance of the proposed trigeneration system

Parameter	Value	Unit
Total energy input to the system	11.644	MW
Total exergy input to the system	11.704	MW
Fuel consumption	0.17	kg/s
Net electric power generated	1011	kW
Cooling capacity	858	kW
Mass flow rate of produced hot water	15.55	kg/s
Total energy efficiency	43.3	%
Total exergy efficiency	10.55	%
Total capital cost rate	37.98	$/hr
Total exergy destruction cost rate	122.25	$/hr
Overall exergoeconomic factor	23.7	%
Total cost rate	160.23	$/hr

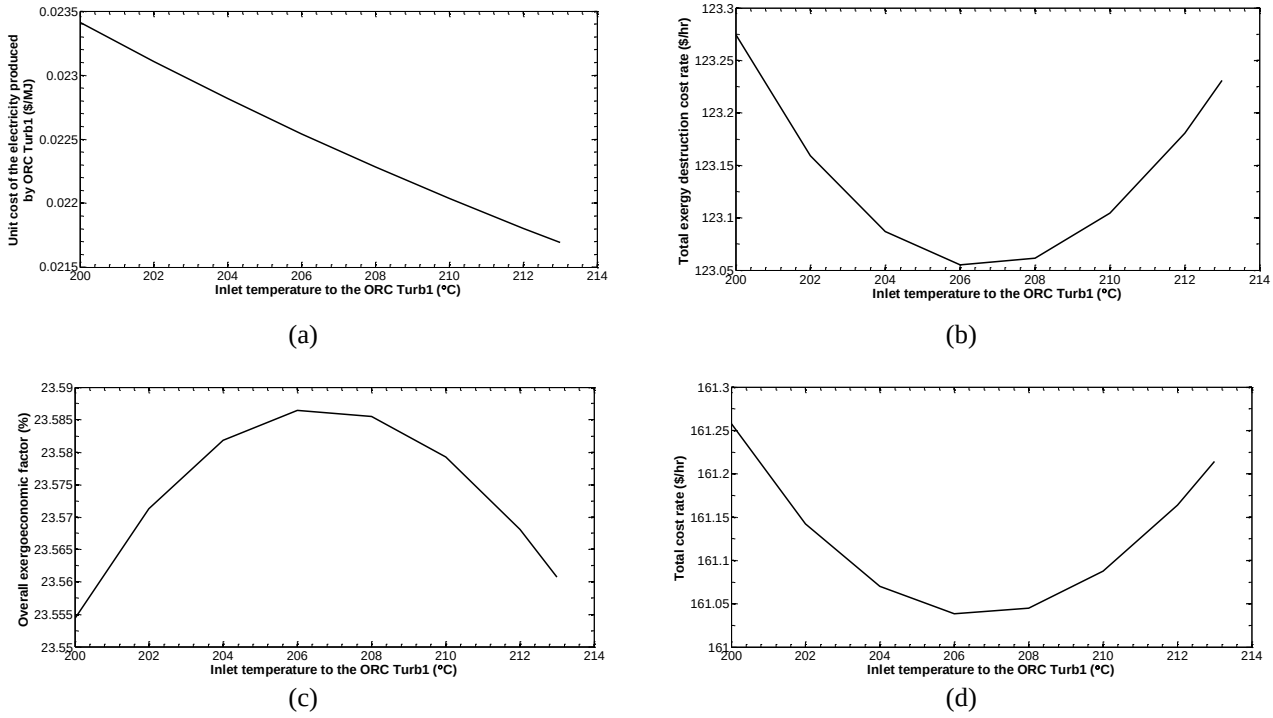

Fig. 6. Effects of ORC Turb1 inlet temperature on (a) unit cost of electricity produced by ORC Turb1, (b) total exergy destruction cost rate, (c) overall exergoeconomic factor and (d) total cost rate (T_{15} = 55 °C, T_4 = 165 °C, P_{24} = 22 bar).

decrease and then increase in the ORC Ex exergy destruction cost rate as T_{13} increases. Note that the exergy destruction cost of ORC Ex constitutes about 54.1% of the total exergy destruction cost rate according to Table 10 and Table 11.

Fig. 6c illustrates the variation of $f_{overall}$ with $T_{13}$and expresses that the value of $f_{overall}$ is maximized at a particular temperature T_{13}. This Fig.indicates that an increase in T_{13}leads to anincrease and then decrease in $f_{overall}$ due to a decrease and then increase in $\dot{C}_{D,total}$ as T_{13} increases based on Fig. 6b.Also the variation of total cost rate,$\dot{C}_{total}$, which is the sum of the $\dot{Z}_{total}$plus$\dot{C}_{D,total}$,withT_{13} is shown in Fig. 6d. The trend is expected consideringthe discussions for Fig. 6b and c.

A similar procedure can be extended for investigating the variations of mentioned exergoeconomic parameters with T_{17}. The observed trends and the corresponding explanations are closely similar to that described by Fig. 6, so they are not demonstrated to avoid repetitiousness.

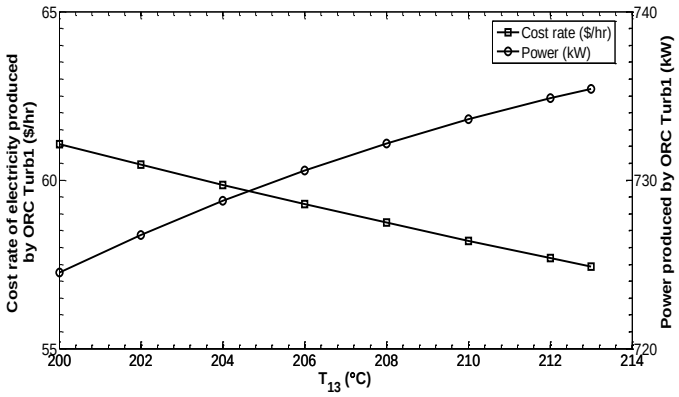

Fig. 7. Variation of ORC Turb1 power and the associated cost flow rate versus inlet temperature of the turbine

Variations of the four above indicated exergoeconomic parameters with T_{15} are shown in Fig. 8. It can be observed inFig. 8a that an increase in condenser temperature leads to adecrease in c_{60}, because of an increase in $\dot{X}_{60}$and, so, a decrease in $\dot{X}_{61}$ as T_{15} increases.

It is seen in Fig. 8b that the exergy destruction cost rate is maximized at particular value of T_{15}. The reason is that, as T_{15} increases, the mass enthalpy difference of the R600a across the ORC Ex decreases while its mass flow rate increases. The net effect is the increment and then decrement of the ORC Ex exergetic efficiency as T_{15} increases. The variation of exergy destruction and its associated cost are proportional to the exergetic efficiency variation.

As Fig. 8b describes, for some value of T_{15}, a maximum value is attained for $\dot{C}_{D,total}$. When $\dot{C}_{D,total}$ has a maximum value, the value of $f_{overall}$ is minimized (see Fig. 8c). The variation of $\dot{C}_{total}$ with T_{15} is also depicted in Fig. 8d. The observed variation is expected according to the results presented in Fig. 8b and c.

The variations of several exergoeconomic parameters with T_4 are presented in Fig. 9. The heat transferred to the power cycle by ORC Ex is decreased with increase in T_4. Therefore, the produced power by the Turb1 and its average cost per unit exergy are changed decreasingly and increasingly respectively based on Fig. 9a.

The effect of T_4 on $\dot{C}_{D,total}$ is indicated in Fig. 9b, which describes an increase of $\dot{C}_{D,total}$ as T_4 increases. As T_4 increases, the value of heat transferred to the R600a in the

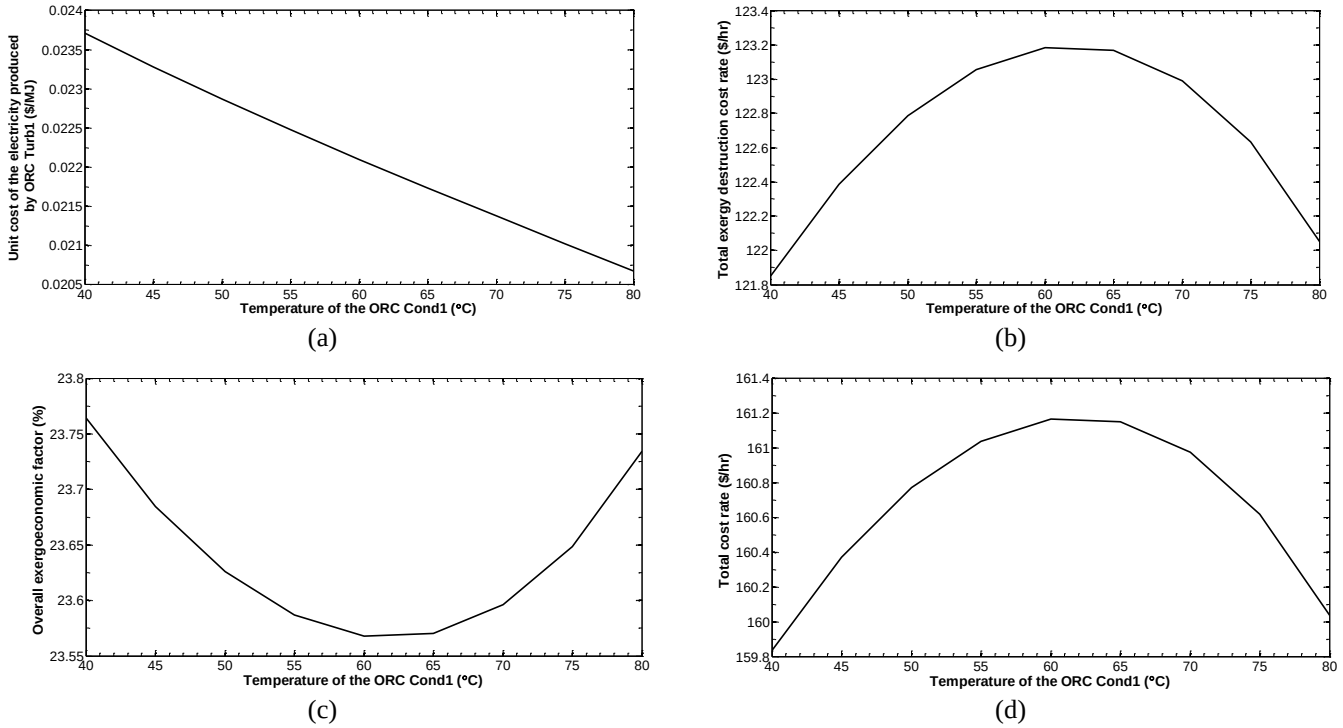

Fig. 8. Effects of ORC Cond1 outlet temperature on (a) unit cost of electricity produced by ORC Turb1, (b) total exergy destruction cost rate, (c) overall exergoeconomic factor and (d) total cost rate (T_{13} = 206.5 °C, T_4 = 165 °C, P_{24} = 22 bar).

ORC Ex decreases and, consequently, the R600a flow rate is reduced. However, as a result, the both values of Feed and Product exergies of ORC Ex are reduced, but, altogether, the exergy destruction and its associated costs are increased as a net effect.

An increase in T_4 leads to an increase in total exergy destruction cost rate. Therefore, increasing T_4 decreases the overall exergoeconomic factor, as illustrated in Fig. 9c. The variation of T_4 increasingly, causes increments of $\dot{C}_{D,total}$ and, so, $\dot{C}_{total}$ as Fig. 9d demonstrates.It is evident that the

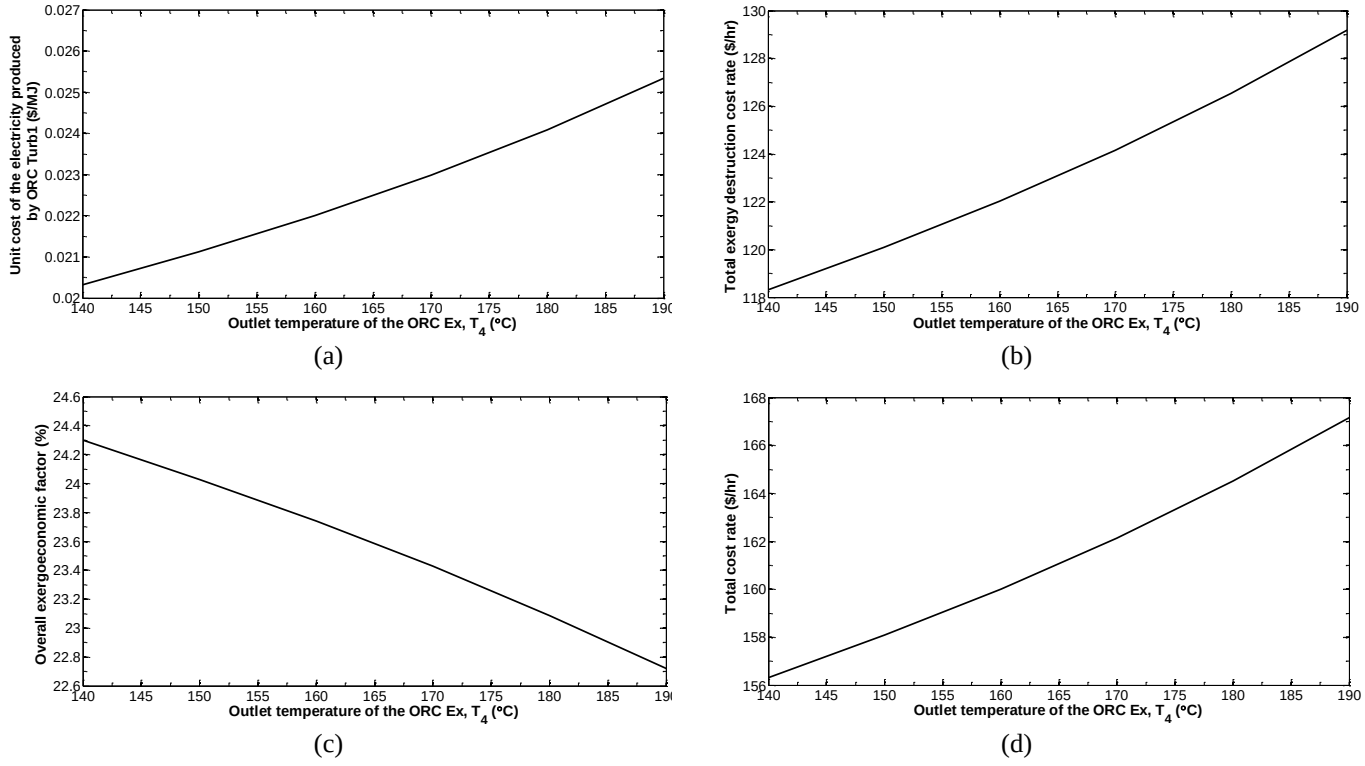

Fig. 9. Effects of ORC Ex outlet temperature, T_4, on (a) unit cost of electricity produced by ORC Turb1, (b) total exergy destruction cost rate, (c) overall exergoeconomic factor and (d) total cost rate (T_{13} = 206.5 °C, T_{15} = 55 °C, P_{24} = 22 bar).

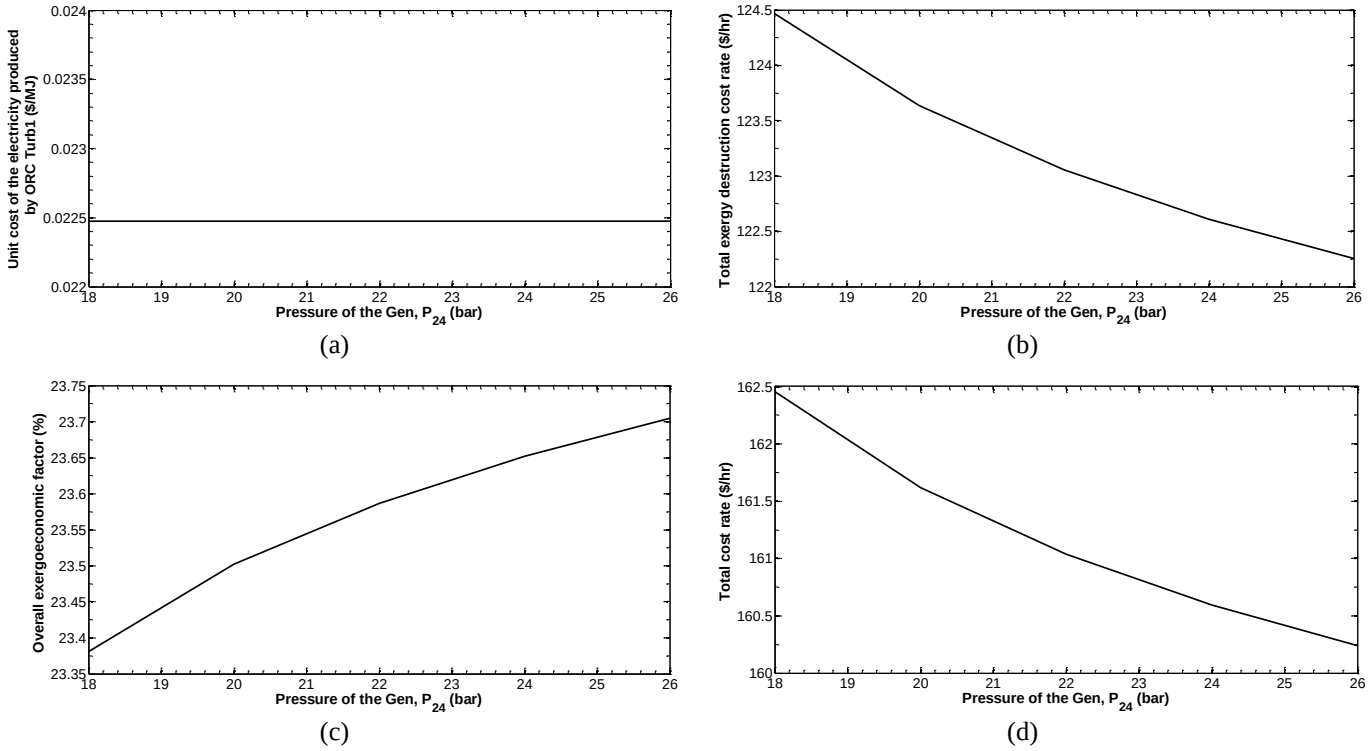

Fig. 10. Effects of operating pressure of cooling cycle, P_{24}, on (a) unit cost of electricity produced by ORC Turb1, (b) total exergy destruction cost rate, (c) overall exergoeconomic factor and (d) total cost rate (T_{13} = 206.5 °C, T_{15} = 55 °C, T_4 = 165 °C).

variation in P_{24} has no effect on the produced power by the ORC Turb1, as shown in Fig. 10a. Based on Fig. 11, by raising the P_{24}, the exergy destructions of Gen and Boiler reduce. Therefore, a decrement of the cost rate associated with exergy destruction is obtained for these two components. According to Table 10, the mentioned components play a significant role in the determination of $\dot{C}_{D,total}$ among the other components of the system affected by P_{24} variation due to their high values of exergy destructions, so the $\dot{C}_{D,total}$ is decreased by P_{24} increment as Fig. 10b presents.

Fig. 10c shows that an increase in the P_{24} results in a smooth increment of the $f_{overall}$. This is because of $\dot{C}_{D,total}$ domination in the denominator of $f_{overall}$ calculation formula and its decrement asP_{24} increases based on Fig. 10b.

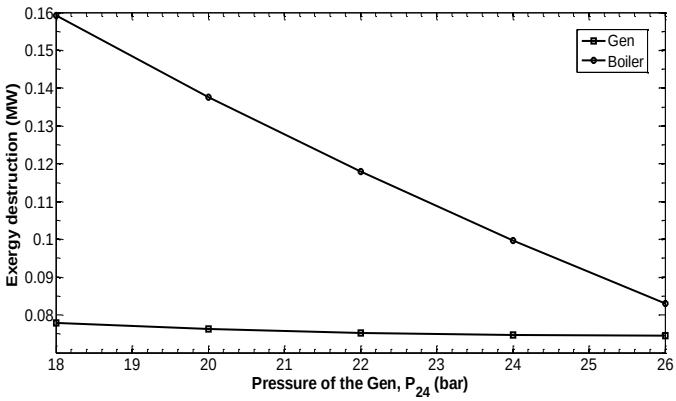

Fig. 11. Exergy destruction variations of two significant components of the cooling cycle versus P_{24}

The summation of $\dot{Z} + \dot{C}_D$ for Gen plus that for Boiler, which is about 5.9 $/hr, expresses the significant influence of these two components on the final value of $\dot{C}_{total}$. Therefore, considering the discussions for Fig. 10b, the variations of $\dot{C}_{total}$ versus P_{24} illustrated in Fig. 10d, are expected. Note that the other components with higher values of $\dot{Z} + \dot{C}_D$ such as ORC Ex, Turb2, Solar Field, Aux and etc are not affected by the variation of P_{24}.

Finally the effects of T_4 and P_{24} on the performance of the whole system are investigated simultaneously and the outcomes are demonstrated by the Fig. 12. As Fig. 12a expresses, for a constant value of P_{24}, an increase in T_4 leads to an increase in the cooling power produced by the cooling cycle of the proposed trigeneration system. The reason is the higher value of heat transferred to the cooling cycle by the Boiler component, as T_4 increases. This Fig. also shows that the lower values of P_{24} cause the higher values of total cooling power generated by the system due to the higher values of flow rate ofrefrigeratorfluid (NH_3) produced by the de-absorber, Gen, for a constant input heat to the Boiler.

Fig. 12b indicates the effect of variations of T_4 and P_{24} on the net power produced by the system. Considering a constant value of P_{24}, as the T_4decreases, the net produced electric power increases because of the heat transfer increasing due to the hot stream temperature difference increasing in the ORC Ex component. Also an increase in P_{24}, results in an increase in the net power generated due to the P_{38} increment and, so, the additional power production by the ammonia turbine, Am Turb, of the cooling cycle.

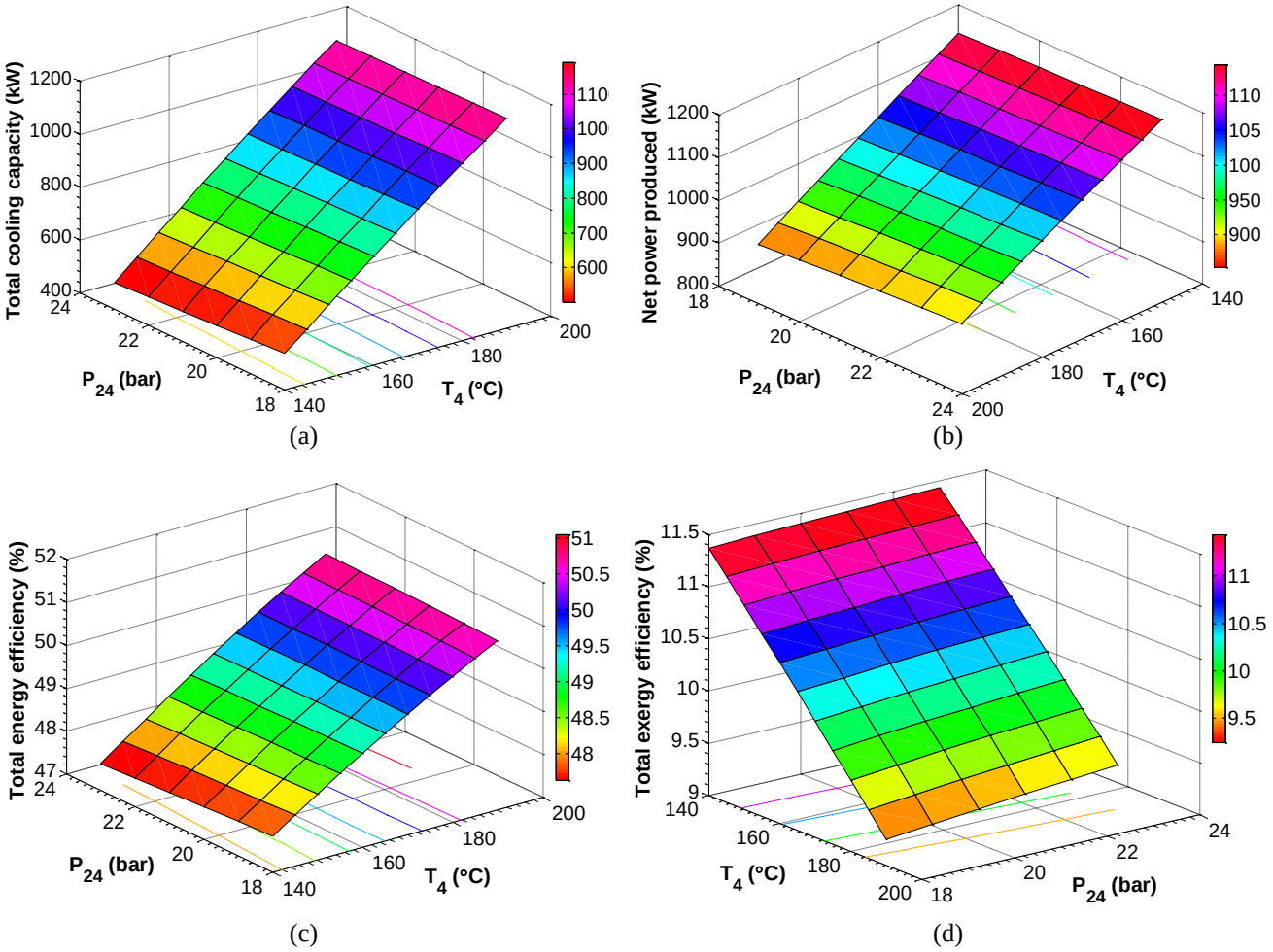

Fig. 12. Effects of T_4 and P_{24} on (a) total cooling capacity, (b) net power produced, (c) total energy efficiency and (d) total exergy efficiency of the system (T_{13} = 206.5 °C, T_{15} = 55 °C).

According to Fig. 12c, total energy efficiency of the system is increased by T_4 increment. On the other hand, the P_{24} has not a significant effect on the total energy efficiency as its variation causes very little variation of η_{total}. It can be realized from this Fig. and Fig. 12a that cooling power generation increment leads to energy efficiency increment of the whole system.

The variations of the total exergy efficiency of system with T_4 and P_{24} are performed by Fig. 12d. Based on this Fig., an exergy efficiency increment is achieved by T_4decrement and P_{24} increment. Therefore, considering Fig. 12a and b, the net power generation increment has a positive effect on ε_{total} increment, but the cooling power increment has a negative effect on it.

5. Multi Objective Optimization

5.1 Problem Definition

For the purpose of system optimization, two objective functions are defined to maximize the exegetic efficiency and minimize the total cost rate of the system simultaneously, so that the exergy destruction and the associated cost rate decrease. Five decision variables are selected based on the mathematical model of the proposed system as they have most effect on the system performance. These five variables and their allowable range of variation are determined by the parametric study of system aspresented in the previous section. So the optimization problem can be described as follows:

$$\text{Maximize } \boldsymbol{\varepsilon}_{\text{total}}(T_{13}, T_{17}, T_{15}, T_4, P_{24}) \tag{34}$$

And

$$\text{Minimize } \dot{C}_{\text{total}}(T_{13}, T_{17}, T_{15}, T_4, P_{24}) \tag{35}$$

Subject to:

$$\begin{cases} 200 \le T_{13} \le 213 \\ 102 \le T_{17} \le 115 \\ 40 \le T_{15} \le 80 \\ 140 \le T_4 \le 190 \\ 18 \le P_{24} \le 26 \end{cases} \tag{36}$$

As an explanation, the selected decision variables are ORC Turb1 inlet temperature (T_{13}), ORC Turb2 inlet temperature (T_{17}), ORC Cond1 outlet temperature (T_{15}), ORC Ex outlet temperature (T_4) and operating pressure of Gen (P_{24}).

A genetic algorithm (GA) programming developed in MATLAB software is used to solve the mentioned multi

objective optimization problem. GA is carried out for 250 generations using a population size of about 300 individuals.

5.2 Optimization *Results*

The value of total exergy efficiency as a function of decision variables is expressed by below expression which is obtained by using GA programming based on the gene mutation probability of 0.4, crossover probability of 0.4and a tournament size of 4:

$$\varepsilon_{total} = 0.02 \times T_{13} - 0.04 \times T_4 + 0.02 \times P_{24} - 5.053 \times 10^{-7} \times [T_4 \times P_{24} - (T_{17} - T_4 + T_{13} \times T_{15}) \times (T_{15} + P_{24} + T_{17}/P_{24})] - 0.02 \times (T_4/T_{17}) + 12.01 \quad (37)$$

Also another expression is achieved for total cost rate evaluation as a GA outcome considering gene mutation probability of 0.5, crossover probability of 0.4and a tournament size of 6:

$$\dot{C}_{total} = 0.0007672 \times (T_{15} + {T_4}^2 - \frac{T_4 - \exp(T_4/P_{24}) + 9.921}{P_{24} - 2.05}) + \frac{30.64 \times (T_{15} - T_{13}/{T_{15}}^2)}{T_4 - 3.442} - (30.64 \times P_{24})/T_4 + 1.753 \times 10^{-5} \times T_{15} \times ({T_{15}}^2 + T_{13} + T_{17} + \exp(T_{17}/P_{24})) + 136.2 \quad (38)$$

The maximum errors for equations (37) and (38) are around4.9% and 2% respectively according to GA report. So based on these equations, the results of system optimization are outlined in Table 12 in whichthe point A introduces the maximization oftotal exergy efficiency,ε_{total}, and the point B presents the minimization of total cost rate, $\dot{C}_{total}$, separately. As Table 12 demonstrates,two decision variables, T_4 and P_{24}, satisfy both objective functions with similar values; but the other decision variables have different values at points A and B. For this reason, 1.03% inevitable increase in optimum (minimum) value of $\dot{C}_{total}$ is obtained when ε_{total} is in optimum conditions, 12.31%, and 8.68% decrease in optimum (maximum) value of ε_{total} is achieved when $\dot{C}_{total}$ is in its optimum value, 153.68 $/hr. Therefore, an optimal operating point, C, is suggested for the purpose of multi objective optimization of the system by a linear approximation to the conditions in which both objective functions are satisfied simultaneously. So, based on the points A and B, the final optimum point is performed by specifying the values of three decision variables, T_{13}, T_{17} and T_{15}; however choosing ofan optimum point, mainly depends on decision maker requirements.

Table 12. The results of multi objective optimization

Optimum parameters	Point A *	Point B **	Point C ***
T_{13} (°C)	213	200	206.5
T_{17} (°C)	115	102	108.5
T_{15} (°C)	80	40	60
T_4 (°C)	140	140	140
P_{24} (bar)	26	26	26
η_{total} (%)	41.91	40.79	41.31
ε_{total} (%)	12.31	11.2	11.72
$\dot{C}_{total}$ ($/hr)	155.27	153.68	155.72

* For maximum exergy efficiency of the system
** For minimum total cost rate
*** Final optimal-point

Moreover, as exhibited in Table 12, it is obvious that high values of total energy and exergy efficiencies cannot guaranty an optimum condition for the system exergoeconomically.

The values of different products of the solar-driven trigeneration system are also given in Table 13 for each optimum points of system. As it seen in this table, the cooling capacity of system is the same for each given points due to the equal values of T_4 and P_{24} for all optimal points.

6. Conclusion

A solar driven trigenerationsystem with theproducts of electricity, refrigerantcapacity and domestic hot water is investigated in this research.A cascade ORC as power generation subsystem and an ammonia turbine within the absorption chiller subsystem are used to increase the total efficiency of system.A quasi-dynamic model developed in MATLABis performed to compute the variations of absorbed solar irradiationinto the Solar Field including PTCs and, so,the temperature of working fluid, water, leaving the Solar Field during the dayby implementation a dynamic link between MATLAB and EES software. Firstly,the optimum length of PTCs is calculated according to the dynamic modeling;exergy and exergoeconomic analysesarethen conducted and system performance is investigated subsequently by applying a parametric study whichemploys the following decision variables:Turb1 and Turb2inlet temperatures, Cond1outlet temperature, ORC Ex hot streamoutlet temperature and Gen pressure. Also a multi objective optimization is reported in order to improve the performance of the system.Several significant observations can be concluded from this study as follows:

- In order, ORC Ex, ORC Turb2, Solar Field and Aux exhibit the highest values of $\dot{Z} + \dot{C}_D$. In contrast, the lowest of this cost rate are for the pumps: P3, P4, P1, P7 and P6.
- The ORC Ex, C.T2, Abs and Ref Cond have the lowest $f_{overall}$ values of below 10% and the highest r_r values among all components of the system. Based on these values, it is resulted that the mentioned components have the worst performances exergoeconomically. Therefore, selecting more expensive components will be helpful in improving the exergoeconomic performance, i.e. higher values of heat transfer area.

- An increase in ORC Ex outlet temperature, T_4, causes an increase in the unit cost of produced power by ORC Turb1, $\dot{C}_{D,total}$ and $\dot{C}_{total}$, and a decrease in overall f when all of the other decision variables remain constant. Also increasing T_4 results in increment of system cooling capacity and totalexergy efficiency, and decrement of net produced power and total energy efficiency.
- The value of $f_{overall}$is maximized and the values of $\dot{C}_{D,total}$ and $\dot{C}_{total}$ are minimized at the particular vales of T_{13}.
- At the particular values of T_{15}, $f_{overall}$ is minimized and, $\dot{C}_{D,total}$ and $\dot{C}_{total}$ are maximized.
- An increase in the pressure of the Gen, P_{24}, leads to a decrease in the total cost rateand an increase in the overall f and total exergy efficiency. In addition,the variation of P_{24} has not a significant effect on the total energy efficiency of the trigeneration system.
- The value of overall exergoeconomic factor for the whole system is observed to be 23.7%, indicating that 76.3% of the total costs are associated with the exergy destruction.
- The multi objective optimization study using GA reveals an 11.1% increase in total exergy efficiency and 2.8% decrease in total cost rate as compared to the non-optimized system (the base case). Moreover, the net generated power is enhanced by 14.38% andrefrigeration capacity of the system is diminished by 43.94% at the optimum conditions.

References

[1] B. Choudhury, B.B. Saha, PK. Chatterjee, JP. Sarkar,"An overview of developments in adsorption refrigeration systems towards a sustainable way of cooling", Applied Energy, vol. 104, pp. 554-567, 2013.
[2] CA. Balaras, G. Grossman,HM. Henning, CA. Infante-Ferreira, E. Podesser, L. Wang, et al,"Solar air conditioning in Europe - an overview", Renewable and sustainable energy reviews, vol. 11, pp. 299-314, 2007.
[3] CS. Solanki,Solar Photovoltaic Technology and Systems, vol. 1. PHI Learning Pvt. Ltd., 2013,pp. 23-24.
[4] International Energy Agency, Technology Roadmap: Concentrating Solar Power, OECD Publishing, 2010.
[5] F. Al-Sulaiman, I. Dincer, F. Hamdullahpur,"Thermoeconomic optimization of three trigeneration systems using organic Rankine cycles: Part I - Formulations",Energy Conversion and Management, vol. 69, pp. 199-208, 2013.
[6] R. Buck, S.Friedmann,"Solar-assisted small solar tower trigeneration systems", Journal of Solar Energy Engineering, vol. 129,pp. 349-354, 2007.
[7] G. Bizzarri, G.L.Morini,"New technologies for an effective energy retrofit of hospitals", Applied Thermal Engineering, vol. 26, pp. 161-169, 2006.
[8] M. Medrano, A.Castell, G. Fontanals, C. Castellón, L.F. Cabeza,"Economics and climate change emissions analysis of a bioclimatic institutional building with trigeneration and solar support", Applied Thermal Engineering, vol. 28, pp. 2227-2235, 2008.
[9] H.W. Prengle, J.C. Hunt, C.E. Mauk,"Solar energy with chemical storage for cogeneration of electric power and heat", Solar Energy, vol. 24, pp. 373-384, 1980.
[10] S. Moustafa, W.Hoefler, H. El-Mansy, A.Kamal, D.Jarrar, H.Hoppman, et al,"Design specifications and application of a 100kWe (700kWth) cogeneration solar power plant", Solar Energy, vol. 32, pp. 263-269, 1984.
[11] S. Göktun, S.Özkaynak,"Performance parameters for the design of a solar-driven cogeneration system", Energy, vol. 26, pp. 57-64, 2001.
[12] G. Mittelman, A.Kribus, A.Dayan,"Solar cooling with concentrating photovoltaic/thermal (CPVT) systems", Energy Conversion and Management, vol. 48, pp. 2481-2490, 2007.
[13] S. Göktun,"Solar powered cogeneration system for air conditioning and refrigeration", Energy, vol. 24, pp. 971-977, 1999.
[14] A.C. Oliveira,"A new look at the long-term performance of general solar thermal systems", Solar Energy, vol. 81, pp. 1361-1368, 2007.
[15] J. Vargas, J. Ordonez, E.Dilay, J. Parise,"Modeling, simulation and optimization of a solar collector driven water heating and absorption cooling plant", Solar Energy, vol.83, pp. 1232-1244, 2009.
[16] H. Alrobaei,"Novel integrated gas turbine solar cogeneration power plant", Desalination, vol. 220, pp. 574-587, 2008.
[17] F.A. Al-Sulaiman, I. Dincer, F. Hamdullahpur,"Exergy modeling of a new solar driven trigeneration system", Solar Energy, vol. 85, pp.2228-2243, 2011.
[18] S. Klein, S. Alvarda, Engineering equation solver (EES). F-chart software, WI, 2007.
[19] S. kalogirou, solar energy engineering: processes and systems, UK:Elsevier, 2009.
[20] H.M. Güven, R.B. Bannerot,"Determination of error tolerances for the optical design of parabolic troughs for developing countries", Solar Energy, vol. 36, pp. 535-550, 1986.
[21] A.V. Arasu, T. Sornakumar,"Performance Characteristics of ParabolicTrough Solar Collector System forHot Water Generation", International Energy Journal, vol. 7, 2006.
[22] R. Forristall, Heat transfer analysis and modeling of a parabolic trough solar receiver implemented in engineering equation solver, National Renewable Energy Laboratory, 2003.

Table 13. Output results of the system based on the optimum points

Optimum points	Net electric power generated (kW)	Cooling capacity (kW)	Flow rate of produced hot water (kg/s)
Point A	1225.8	480.97	15.55
Point B	1095.3	480.97	15.55
Point C	1156.4	480.97	15.55

[23] A.Y. Cengel, M.A.Boles, Thermodynamics: An engineering approach, New York:McGraw Hill, 2008.
[24] F.P. Incropera,Introduction to heat transfer, New York:John Wiley & Sons, 2011.
[25] B.R. Munson, D.F.Young, T.H. Okiishi, Fundamentals of fluid mechanics, 6th ed., New York:John Wiley & Sons, 2009.
[26] S.R. Turns, An introduction to combustion, New York:McGraw-hill, 1996.
[27] T.J. Kotas, The exergy method of thermal plant analysis, Reprint ed., Malabar:Krieger Pub., 1995.
[28] A. Bejan, G. Tsatsaronis, M.J. Moran, Thermal design and optimization, New York:John Wiley & Sons Inc., 1996.
[29] I. Dincer, M.A. Rosen, Exergy: energy, environment and sustainable development,2nd ed., UK:Elsevier, 2012.
[30] A.G. Kaviri, M.N.M. Jaafar, T.M.Lazim,"Modeling and multi-objective exergy based optimization of a combined cycle power plant using a genetic algorithm", Energy Conversion and Management, vol. 58, pp. 94-103, 2012.
[31] C. Zamfirescu, I.Dincer,"How much exergy one can obtain from incident solar radiation?", Journal of Applied Physics, vol. 105, pp. 044911, 2009.
[32] F. Mohammadkhani, N. Shokati, S. Mahmoudi, M.Yari, M.Rosen,"Exergoeconomic assessment and parametric study of a Gas Turbine-Modular Helium Reactor combined with two Organic Rankine Cycles", Energy, vol. 65, pp. 533-543, 2014.
[33] H.P. Loh, J. Lyons, Process Equipment Cost Estimation, DOE/NETL, National Energy Technology Center, 2002.
[34] P. Ahmadi, I.Dincer,"Exergoenvironmental analysis and optimization of a cogeneration plant system using Multimodal Genetic Algorithm (MGA)", Energy, vol. 35, pp. 5161-5172, 2010.
[35] G. Tsatsaronis, J.Pisa,"Exergoeconomic evaluation and optimization of energy systems - application to the CGAM problem", Energy, vol. 19, pp. 287-321, 1994.

Nomenclature

A	Area (m^2)
abs	Absolute pressure symbol
B	Aperture of the parabola (m)
$\dot{C}$	Cost rate ($/hr or $/s)
CRF	Capital recovery factor
c	Average cost per unit exergy ($/MJ)
EPC	Equipment purchase cost ($)
f	Exergoeconomic factor
f_f	Friction factor
h	Specific enthalpy (kJ/kg)
h_a	Hour angle (°)
h_{cnv}	Convection heat transfer coefficient (kW/m^2-K)
Irr	Solar irradiation (kW/m^2)
LHV	Low heating value of fuel (kJ/kg)
L_l	Cylinder length (m)
L_{tot}	Total length of PTCs per each row (m)
MW	Molecular weight (kg/kmol)
$\dot{m}$	Mass flow rate (kg/s)
P	Pressure (bar)
Pl	Parallel rows of PTCs
Q	Heat rate (kW)
R	Gas constant (kJ/kmol-K)
r	Radius (m)
r_r	Relative cost difference
s	Specific entropy (kJ/kg-K)
T	Temperature (°C or K)
V	Velocity (m/s)
$\dot{X}$	Exergy (kW or MW)
x	Specific exergy (kJ/kmol)
y	Molar fraction
$\dot{W}$	power (kW)
$\dot{Z}$	Investment, operating and maintenance cost rate ($/hr)

Subscripts

0	Ambient/Dead state
1, 2, 3, …	Cycle locations
c	Coating
CH	Chemical
col	Solar collector
cnd	Conduction heat transfer
cnv	Convection heat transfer
D	Destruction
DHW	Domestic hot water
F	Feed
f	Fuel
fl	Fluid
g	Glass cover
HE	Heat exchanger
i	Inlet/Inner
ic	Inner cylinder
k	Component of mixture
KN	Kinetic
m	Mean
o	Outlet/Outer
oc	Outer cylinder
P	Pump
PH	Physical
PT	Potential
p	Product
Q	Boundary heat transfer
Ref	Refrigeration
rad	Radiation heat transfer
sol	Solar
W	Boundary mechanical work

Greek symbols

α	Solar altitude angle (°)
α_a	Absorptance coefficient
Δ	Difference between inlet and outlet
ε	Exergy efficiency
ε_e	Emissivity
η	Energy efficiency
η_{opt}	Optical efficiency
γ	Maintenance factor
ρ	Density (kg/m^3)
ρ_{cl}	Reflectivity of the reflectors of PTCs in clean conditions
Ω	Correction factor of the optical efficiency
ω	System operating hours per year (hr)
τ	Transmittance coefficient
δ	Declination angle (°)
θ	Incidence angle (°)
σ	Stefan–Boltzmannconstant

Components Abbreviation

Abs	Absorber

Am Cond	Ammonia Condenser
Am Ex	Ammonia Heat Exchanger
Am Turb	Ammonia Turbine
Aux	Auxiliary Unit
Cond	Condenser
C.T	Cooling Tower
Evap	Evaporator
Gen	Generator
HR Ex	Heat Recovery Heat Exchanger
ORC Ex	ORC Heat Exchanger
P	Pump
PTCs	Parabolic Trough Collectors
Ref Cond	Reflux Condenser
Sol Ph	Solution Preheater
Sprtr	Separator
Turb	Turbine
Valve	V